

STAT 2

Ru 88
5141

Statistical Aspects of Ice Gouging on the Alaskan
Shelf of the Beaufort Sea

by

W.F. Weeks¹, P.W. Barnes², D.M. Rearic² and Erk Reimnitz²

1. U.S. Army Cold Regions Research and Engineering Laboratory,
72 Lyme Road
Hanover, NH 03755
2. Pacific-Arctic Branch of Marine Geology
U.S. Geological Survey
345 Middlefield Road (MS99)
Menlo Park, CA 94025

Abstract.

The statistical characteristics of the ice produced gouges **that** occur on the sea floor along a 190 km stretch of the Alaskan coast of the **Beau-**fort Sea between Smith Bay and Camden Bay are studied. The data set is based **on** 1500 km of precision **fathometry** and side-looking sonar records that were obtained between 1972 and 1979 in water depths to 38 m. The probability density function of the gouge depths into the sediment can be represented by a simple negative exponential over 4 decades of gouge frequency. The exceedance probability function is, therefore, $e^{-\lambda d}$ where d is the gouge depth in meters and λ is a constant. The value of λ shows a general decrease with increasing water depth **from** 9 m^{-1} in shallow water to **less** than 3 m^{-1} in water 30 to 35 m deep. The deepest gouge observed was 3.6 m from a sample of 20,354 gouges that have depths of greater or equal to 0.2 m. The dominant gouge orientations are usually **unimodal** and reasonable clustered, with the most frequent **alignments** roughly parallel to the general trend of the coastline. The value of \bar{N}_1 , the mean number of gouges (deeper than 0.2 m) per kilometer measured normal to the trend of the gouges, varies from 0.2 for the protected lagoons and sounds **to** 80 in water between 20 and 38 m deep in the unprotected offshore regions. The

distribution of the spacings between gouges as measured along a sampling track is a negative exponential. The form of the frequency distribution of N_1 varies with water depth and is exponential for the lagoons and sounds and shallow offshore areas, positively skewed for 10 to 20 m depths off the barrier islands, and near-normal for deeper water. As a Poisson **distribu-**tion gives a reasonable fit to **the N_1** distributions for **all** water depths, **it** is suggested that gouging can be taken as approximating a Poisson process in both space and time. The distributions of the largest values per kilometer of gouge depths, gouge widths and the heights of the lateral embankments of sediments plowed from the gouges are also investigated. Limited data on gouging rates give an average of 5 gouges per kilometer per year. Examples are given of the application of the data set to hypothetical design problems associated with the production of **oil** from areas in the Alaskan portion of the Beaufort Sea.

I. INTRODUCTION

A survey of the **bathymetry** of the **Beaufort** Sea shows that **large** areas of this marginal sea of the Arctic Ocean have water depths of less than 60 **m**. It **is** now known that in this region ungrounded pressure ridge keels may protrude downward for nearly 50 meters and that ice floes containing such keels drift in a general pattern from east to west along the Beaufort coast. Therefore **it** is reasonable to presume that such sea ice masses could interact with the sea floor. Indeed, ice-related disturbances of the sea floor have been inferred for some decades from observations of sea floor sediments entrained **in** obviously grounded ice masses (Kindle, 1924). As such processes were, at the time, **largely** of academic interest, there was **little** motivation to systematically explore them further.

With the discovery of oil and gas along the margins of the Beaufort Sea at **Prudhoe** Bay and off the Mackenzie Delta, processes modifying the floor of the Beaufort Sea became of interest due to their possible effect on offshore design and operations. Examination of early side-scan sonar and precision fathometry data coupled with diving observations (Shearer et al., 1971; **Pelletier** and Shearer, 1972; Kovacs, 1972) showed **clearly that** much of the sea floor was heavily marked by long linear depressions, which we will refer to as gouges, produced by the **ploughing** action of ice. The depths and widths of gouge incisions in the sea floor reached several meters and several tens of meters respectively, with gouges occurring as both individual isolated events and as multiple events presumably produced by projections on the same pressure ridge keel gouging the sea floor as

part of **the** same ice motion (**Kovacs** and **Mellor**, 1974; **Reimnitz** and Barnes, 1974).

In the present paper we will discuss some statistical aspects of the ice-produced gouges that occur along a 190-km stretch of the coast of the Alaskan Beaufort Sea between Smith Bay and Camden Bay. [Figure 1 is included to assist one in locating the various bays, points and islands along the Beaufort **Coast.**] We will also include a brief discussion of the statistical concepts and techniques that are utilized. As much of the study area is part of the 1979 and 1982 lease sales offered by the State of Alaska and the Federal Government, we believe that the results reported here hold immediate interest to the engineering community involved in off-shore design for the **Beaufort** Sea as **well** as long-term interest to the scientific community interested in near-shore processes in shallow, **ice-**covered seas. Therefore the paper is concluded by discussing some of these potential applications.

II. BACKGROUND AND ENVIRONMENTAL SETTING

Because of their importance to offshore design in arctic areas, **ice-**produced gouges have been the subject of a number **of** investigations, especially since the time when they were recognized as a recurring sea-floor feature in the shallow portions of ice-covered seas. Rather than review this literature here, we will simply mention publications of general interest that can be used to find more exhaustive reference lists. Reviews of early work can be found in Kovacs (1972) and Kovacs and **Mellor** (1974). Early studies off the Mackenzie **Delta** are described by Shearer et al. (1971); **Kovacs** and **Mellor**, 1974; and by **Pelletier** and Shearer (1972).

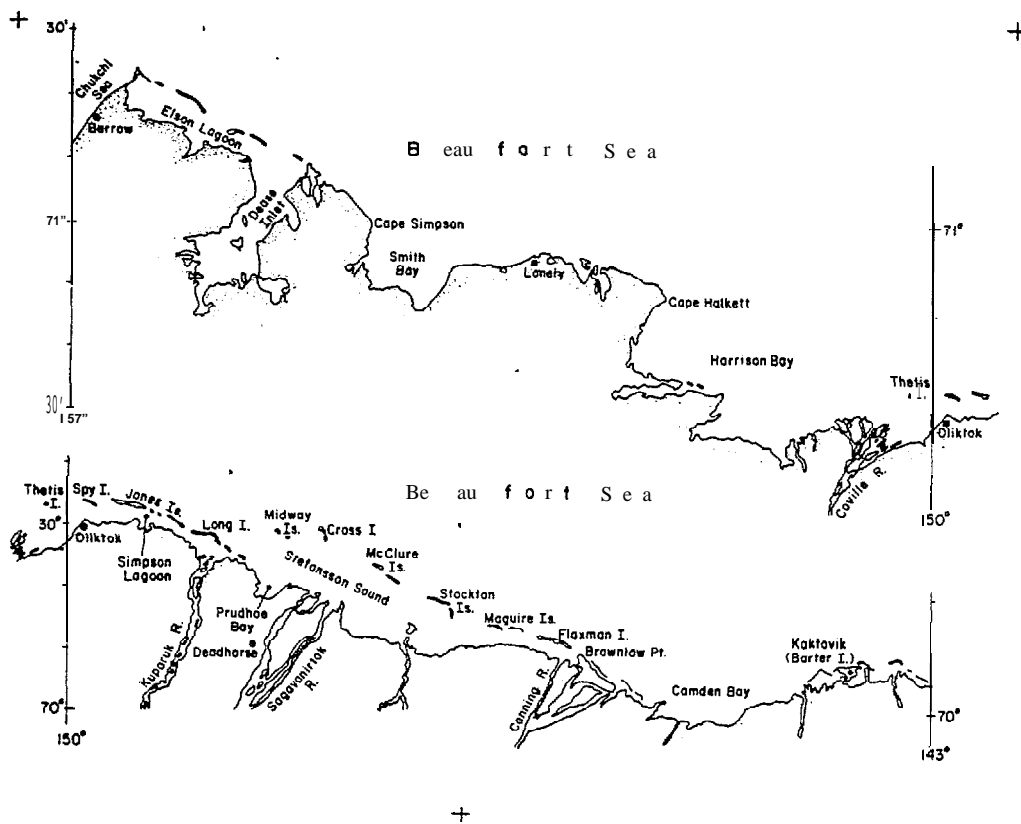


Figure 1. Map of a part of the Alaskan coastline of the Beaufort Sea giving place names mentioned in text.

Early work off the Alaskan coast is reported by Skinner (1971), **Reimnitz** et al. (1972, 1973), Barnes and **Reimnitz** (1974), and **Reimnitz** and Barnes (1974). More recent work is discussed by Shearer and **Blasco** (1975), **Reimnitz** et al. (1977 a, b; 1978), Barnes et al. (1978), **Hnatiuk** and Brown (1977), and Barnes and **Reimnitz** (1979). These studies provide the reader with a description of the nature of the gouges, the characteristics of the Ice involved in the gouging process, the general distribution of gouging along the coast, and, to some extent, the forces involved in the process and the rates of gouge recurrence. In most studies little attention was paid to ways that the observed gouge parameters varied or to methods for estimating infrequent gouging events, such as the formation of deeper gouges. Exceptions to this are the papers by Lewis (1977 a, b) and **Wahlgren** (1979 a, b), in which the statistical aspects of the gouges located in the general area of the Mackenzie Delta are examined.

Present evidence suggests that the Beaufort Sea shelf has been relatively stable during the last 10,000 years (*i.e.* major tectonic or **glacio-isostatic** adjustments have **not taken** place (Hopkins, 1967). As sea level has risen approximately 35 m in this time period, the entire sea **floor** of the present study area was land in the geologically recent **past**. The gentle slope of the present land surface continues **northward** to a water depth of 60 to 70 m where the **shelf** break occurs (Barnes and Reimnitz, 1974). Figure 2 gives generalized **bathymetry** for the study area. The broad gently sloping shelf **is** quite evident. If the sea floor topography in the study area is examined in more detail it is found to be very complex (see **map** given as Appendix A). The most notable features are a number of

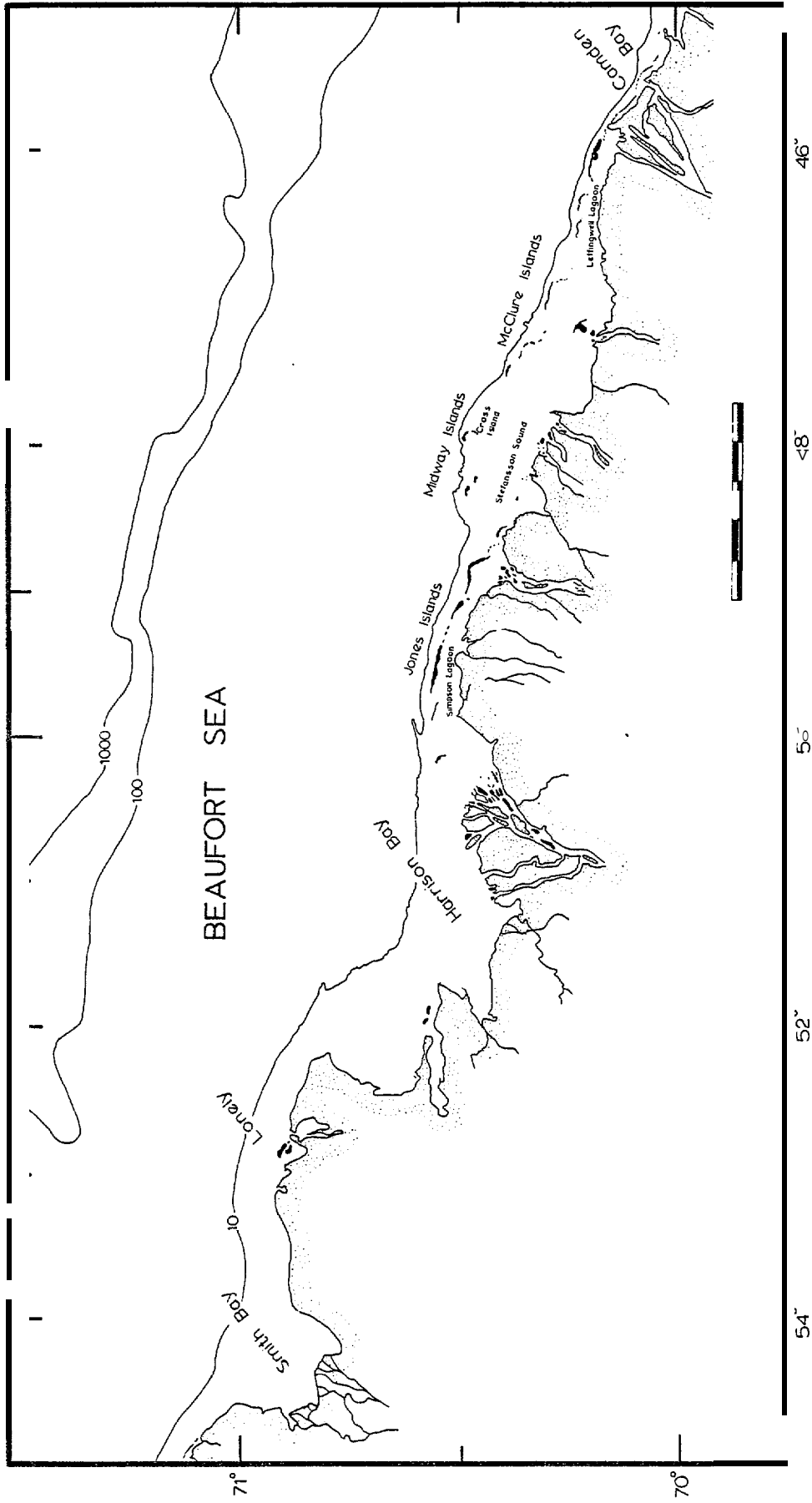


Figure 2. Generalized bathymetric chart of the study area.

submerged shoals and bottom irregularities which have been related to ice zonation (Reimnitz et al., 1977b). On the scale of the gouging it is even more complex (not shown). Holocene sediments (chiefly poorly sorted silty clays and sandy muds) exhibit maximum thicknesses of 5 to 10 m over the inner shelf. The seabed of the region is characterized by extreme diversity and variability of sediment types, seabed character, and sedimentary structures. Sedimentary structures are dominated by wave- and current-related processes inshore of 10 m, by ice- and ~~wave-~~ and current-related processes between 10 and 20 m, and by primarily ice related processes out to water depths of 50 m or more where water-related **depositional** processes again dominate. Noteworthy is the nearly ubiquitous occurrence of stiff silty clays in outcrops on the inner shelf.

The oceanographic **regime** of the region has been **little** studied. The near-shore circulation appears **to** be strongly wind-driven during the summer, with flushing rates and currents closely related to local winds. The most striking oceanographic events are waves, currents and surges resulting from **late** summer storms. **Local** sea **level** rises of 3-m coupled with 3-m waves have been observed. Limited data during the summer suggest a general westward water motion produced by the prevailing easterlies, but wind-driven reversals are not rare. During the winter the dominant currents on the inner shelf are believed to be the **result** of **thermohaline** drainage out of the nearshore regime of dense, **cold**, salt-rich water produced by the formation of sea ice (Mathews, 1981).

The ice regime of the region shows great changes with season and distance from shore. During the summer ice conditions are extremely

variable. Much of the study area is commonly ice-free with the southern edge of the **multiyear** pack ice occurring between 10 to 100 kilometers offshore. New **ice** starts to form in October and during the early stages of its formation ice movement velocities nearshore are similar to velocities offshore (5 km/day on the average with highs of 35 km/day during storms (Thomas and Pritchard, 1979)). As the new ice thickens, velocities decrease at nearshore locations **until** the ice becomes **truly** fast experiencing motions of only a few 10s of meters over the remainder of the winter. At offshore locations, motions also decrease somewhat but movements still remain significant (1 to 2 km/day). At times **the whole ice pack may** be nearly motionless for periods of several days. Numerous pressure ridges form in the moving **ice** and in shallower areas many of these ridges become grounded. Areas of particularly heavy grounding occur off the barrier islands in water depths of roughly 20 m. In areas such as Harrison Bay that are not protected by barrier islands, **large** grounded ridges occur in shallower waters (roughly 10 m depth). Once the grounded ridge or **stamukhi** zone develops, the ice shoreward of this feature remains relatively motionless until spring. During spring, which on the coast of the Beaufort Sea occurs in June, melting **allows** formerly bottom-fast ice near the shore to float. This allows the nearshore ice to, once again, become mobile. Many examples of ice pile-up and over-ride on beaches are known to occur during this period. Within the constraints presented by the coast and by grounded ridges and rubble fields, the nearshore ice remains mobile throughout the complete summer unless it disappears by melting or by being blown out to sea. However, the massive areas of grounded ridges and rubble often remain

grounded throughout most or even all of the **summer** (Barnes and **Reimnitz**, 1979). Associated with these grounded ice features at 18 to 20 m water depth is a break in seabed slope and changes in gouge character and in sediment texture (**Reimnitz** and Barnes, 1974). Additional information on the oceanography and **sedimentology** of the study area can be found in APO (1978).

·III. DATA COLLECTION AND TERMINOLOGY

Seven years of data obtained between 1972 and 1979 (excluding 1974) were used in the present study with a **total** sample **trackline** length of approximately 1500 km. Data were collected from the Research Vessels **Loon** and **Karluk**, using a side-scan sonar and a precision fathometer (200 **kHz**). Both systems were capable of resolving bottom relief of less than 10 cm. The sidescan records covered either 200-m or 250-m swaths (depending on scale selection) of sea floor beneath the ship, Figures 3 and 4 show a representative **sonograph** and a **fathogram** respectively. The tracks were spaced to provide fairly **evenly** distributed sampling along the coast between Smith Bay and Camden Bay. Data were obtained both inside and seaward of the barrier islands to the 38-m **isobath**. Figure 5 shows the locations of the different sampling **lines**. The **trackline** navigation was plotted in 1-km segments. The monographs and fathograms were also divided into 1-km segments and correlated directly with the navigation. Some aspects of the data interpretation are subjective. To minimize variations due to this factor, **all** the counting and measuring was performed by one individual (L.I.R.). A complete ice gouge data record sheet showing all measurements is given by Rearic et al. (1981). A description of the general techniques

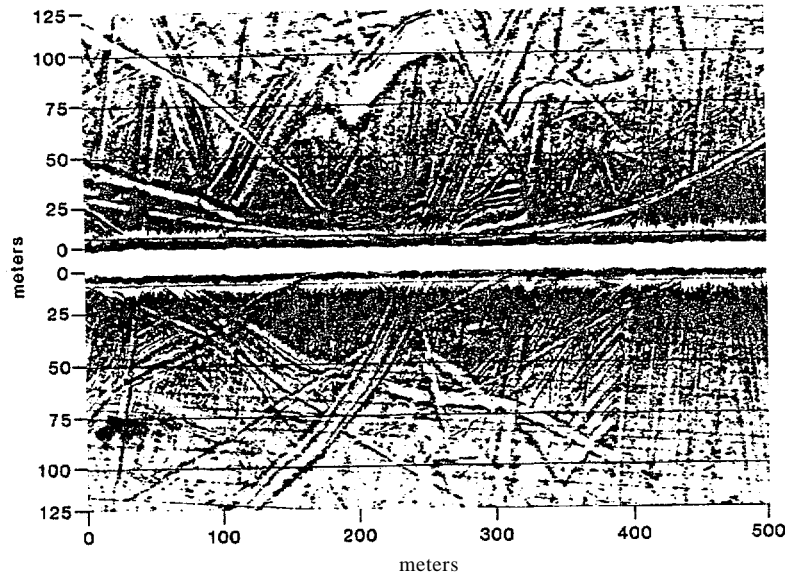


Figure 3. Sonograph of ice gouged seafloor. Water depth is 2011m.
Record taken 20km NE of Cape Halkett.

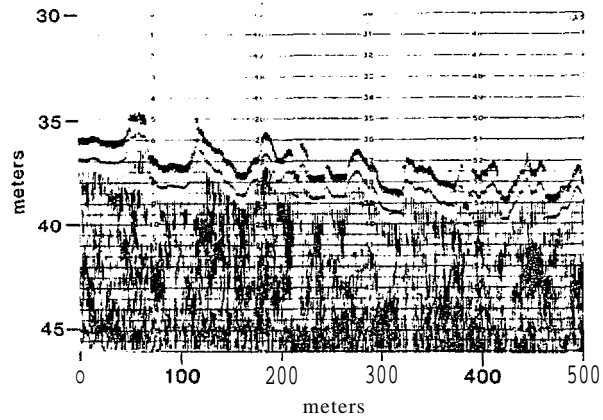


Figure 4. Fathogram of ice gouged seafloor. Water depth is 36m.
Record taken 25km NE of Cape Halkett.



Figure 5. Map showing the location of the sampling lines. The arrows indicate the direction of ship movement.

that were used in analyzing the monographs and fathograms can be found in Barnes et al. (1978). A few important points affecting the parameters used in the present study should be mentioned, however:

average water depth (\bar{z}) - determined by averaging the water depths observed at the start and at the end of each 1-km section; as z changes are usually gradual and reasonably smooth, \bar{z} should be a reasonable approximation to a spatially integrated value.

dominant gouge orientation (θ) - templates were used to remove horizontal exaggeration from the monographs and to obtain all measurements of the estimated dominant orientation to within 5° true. (It should be noted that the gouge orientations within each line segment are variable (see Figure 3).)

spatial gouge frequency (N_1) - in determining the number of gouges per kilometer of sampled track (N) every feature (on the fathogram) presumed to result from ice contact with the bottom was counted, including individual gouges produced by different segments of what was probably the same pressure ridge keel (our interest is in the number of gouges in the bottom, not in the number of ice events); these N values were then corrected in order to estimate N_1 , the expected number of gouges that would have been seen on a 1 kilometer sampling line if the ship's track was oriented normal to the dominant gouge trend. This correction was made by using $N_1 = N/\sin a$ where a is acute angle between the ship track and the gouge orientation. As most gouges are oriented parallel to the coast and the majority of the sampling lines were roughly normal to the coast, these corrections were usually small. Gouges with depths of less than 0.2 m were not counted as

it commonly was difficult to positively identify **all** of these small gouges on the **fathogram**. Actually in the original data tabulations (**Rearic et al., 1981**) a value was given for the number of gouges in the 0 to 0.2 m range that could be distinguished on the sonar record. Although this value can be useful, it should not be combined with the data on gouges deeper than 0.2 m as it includes a large number of gouges that do not cross beneath the ships track (**i.e.** that would not appear on the fathometer track).

gouge depth {d} - the depth measured (on the fathometer track) vertically from the level of the (presumably undisturbed) adjacent sea floor to the lowest point in the gouge (see Figure 6); values were grouped in 20-cm class intervals; in some cases, because of factors such as ground swell and wind chop, it was **only** possible to determine the number of gouges that have depths greater than a specified value; because of these problems gouges having depths of less than 0.2 m were not considered; each individual gouge was measured; also determined was the maximum gouge depth (d_{\max}) observed in each kilometer of sample track; it should be noted that because of **infilling** by sediment, the measured d values are presumably less than the d values at the time the gouge formed.

maximum gouge width (w_{\max}) - this measurement is taken between the inside **walls** of the gouge at the level of the undisturbed surrounding sea floor (see Figure 6); the maximum value in each kilometer of sample track **is** recorded.

maximum lateral embankment height (h_{\max}) - the maximum height (**in** each kilometer of sample track) of the embankments of sediment plowed from

the gouges measured relative to the undisturbed sea floor, (see Figure 6) and occurring along the margins of the gouges.

It should be noted that values of d and h_{\max} are determined purely from the linear **fathometer** profiles. It is, however, known from other data (**sonograms**, dive observations, and repetitive **tracklines**) that both gouge depths and lateral embankment heights can vary considerably along the length of a given gouge.

As is clear from comparing our terms with the titles of papers in our reference list, terminology for ice-induced sea floor features is far from standardized. This should not be a problem as long as individual authors clearly spell out their usage of specific terms. There is little we can do here to resolve terminology disputes. We **would** simply like to point out that gouge and gouging in the present study correspond to scour and scouring in the papers of **Pelletier** and Shearer (1972) and Lewis (1977a,b) and to score and scoring in the papers of **Kovacs** (1972) and **Kovacs** and **Mellor** (1974).

In the analysis the data **will** commonly be combined **into** several different groups based primarily on geographic location. A given group will be referred to by either a geomorphic characteristic common to the group or by the name of a geographic feature occurring within or near the location to the group. To be specific the groups are:

- a) Lagoons and Sounds (lines 2-4, 14, 15; 3-7, 8, 9, 12, 13, 14; 5-3, 12; 8-37, 40, 41),
- b) Lonely (lines 7-39, 40, 41, 42),

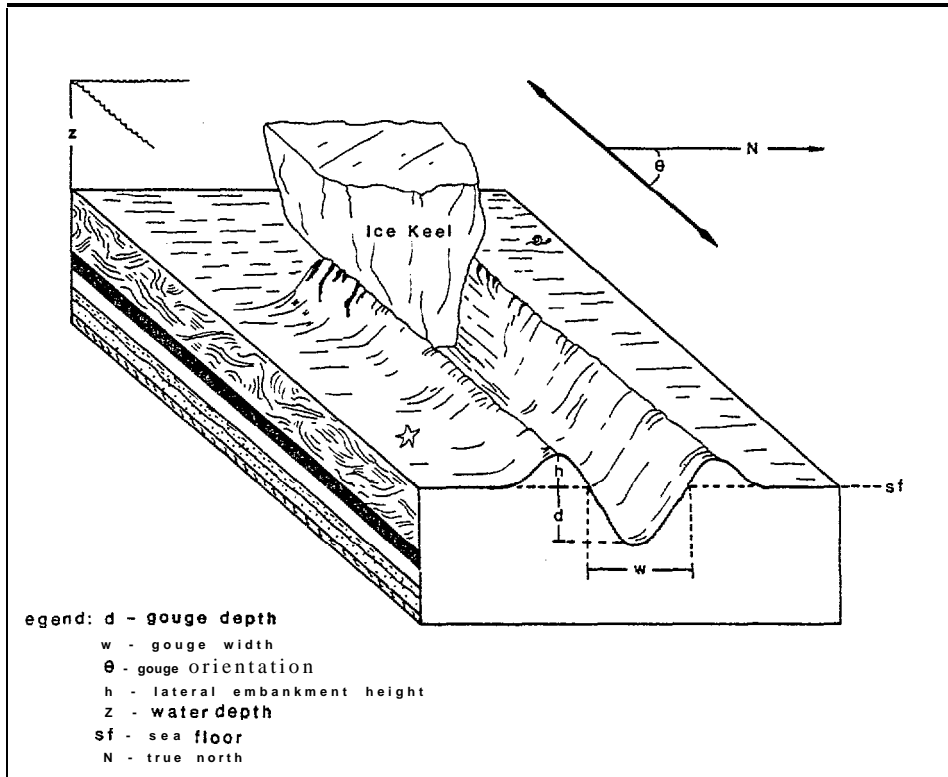


Figure 6. Schematic drawing of a gouge showing the location of several measurements referred to in the text.

- c) Harrison Bay (lines 2-19, 5-12, 6-22, 7-35; note that the ~~near-~~ shore lines 6-20, 21, 23, 24 and 25 were not used as the sonar records indicated sand waves and other features that suggested extensive movement of bottom sediment),
- d) Jones Islands (lines 2-15, 17, 21; 7-31, 66, 67, **71**; 9-92; observations from north of Spy Island to the north of ~~the~~ Midway Islands)
- e) McClure Islands (lines 3-9, 10, **11**, 13, 14; 5-3, 4; 7-76; 9-44, 63, 65, 66, 78; observations from Cross Island to Camden Bay),
- f) Jones Islands and East (a combination of the Jones and the McClure Islands data sets; i.e. **all** the data seaward of the barrier islands and east of Harrison Bay),
- g)** Harrison Bay and East (a combination of the data sets from Harrison Bay, Jones Islands and McClure Islands; i.e. all the data seaward of the barrier islands except the four tracks off of Lonely).

IV . GOUGE DEPTHS

To examine the distribution of gouge depths we prepared histograms of gouge depths for different regions. The nature of these graphs was clearly a decreasing exponential **with** a rapid fall-off in the frequency of occurrence of larger gouges. A similar tendency has been noted by both Lewis (1977 a, b) and **Wahlgren** (1979 a, b) for the gouges occurring north of the Mackenzie **Delta**. However, an examination of their data (Lewis 1977a) shows that the number of small gouges is significantly less than would occur in

an exponential model suggesting that some other type of distribution might also **be** a possibility.

Figure 7 shows a **semilog plot** of the number of gougues with different gouge depths for four representative areas of the study region: (a) from the lagoons and sounds (41 data points), (b) from Harrison Bay (842 data points), (c) from off of Lonely (2869 data points), and (d) from the profiles seaward of the barrier islands and east of Harrison Bay (16620 data points). Other groupings of the data and data from other areas gave similar plots. The four curves are well separated as the result of the coincidence that the numbers of gougues observed in the four regions are quite different. This is the result of differing lengths of sampling **line** and of differing spatial gouge frequencies. If the same sets of data are plotted as relative frequency (the proportion of the total number of observations from that region that occurs in each of the 0.2 m depth classes) the shapes of the curves are identical but there is considerable overlap, Note that all **plots** are reasonably linear over the complete range of four decades [r^2 values vary from 0.94 to 0.98 (r^2 gives **the** fraction of the variation in the number of gougues observed accounted for by the regression line; in this 94 to 98%)]. This suggests that the utilization of an exponential distribution in the Mackenzie studies as suggested by Lewis (1977a) was justified.

The exponential distribution is a convenient, **well** studied distribution (see, among others, Benjamin and Cornell, 1970 and **Miller and Freund, 1977**). If the simple frequency distribution is a negative exponential,

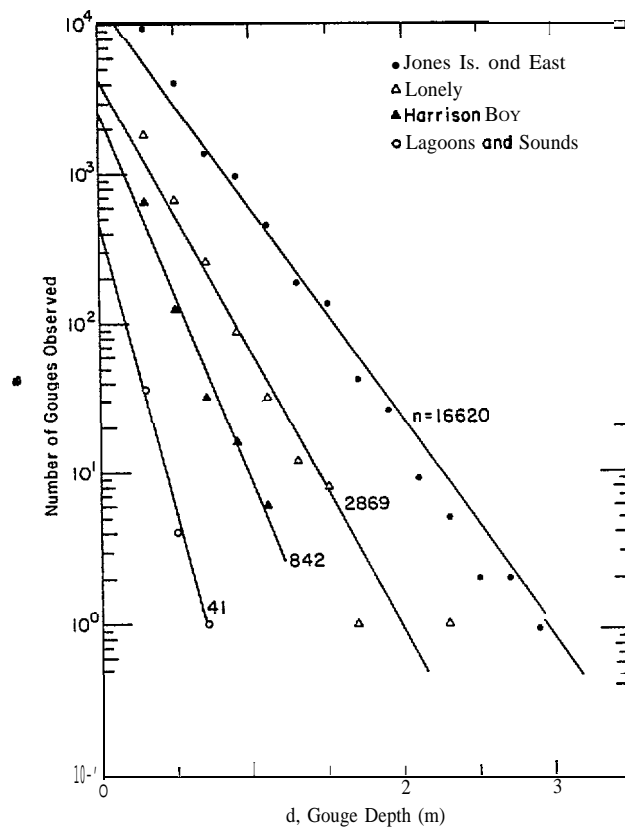


Figure 7. Semilog plot of the number of gouges observed versus gouge depth for 4 regions along the Alaskan coast of the Beaufort Sea.

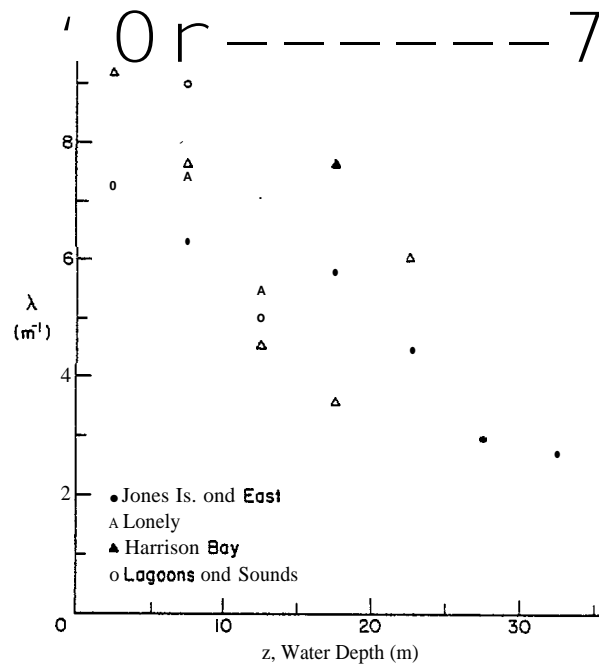


Figure 8. Plot of λ (m^{-1}) versus water depth (z) in meters for 4 different geographic areas along the coast of the Beaufort Sea.

then **the** probability density function (PDF) of X will also be of a similar form

$$f_X(x) = ke^{-\lambda x} \quad x \geq 0$$

(Here x represents the values that the random variable X may acquire.)

Because the integral of $f_X(x)$ from 0 to ∞ **must equal 1**, as **it** contains **all** the sample points with nonzero probabilities,

$$\int_0^{\infty} k e^{-\lambda x} dx = \left. \frac{-k}{\lambda} e^{-\lambda x} \right|_0^{\infty} = \frac{k}{\lambda} = 1$$

or

$$k = \lambda$$

This gives the following PDF

$$f_X(x) = \lambda e^{-\lambda x} \quad x \geq 0 \quad (1)$$

Here the free parameter λ is simply the reciprocal of the sample mean (\bar{x})

$$\lambda = \frac{1}{\bar{x}}$$

The probability **that** a random variable will assume a value in the interval (x_1, x_2) **is then**

$$P[x_1 < X < x_2] = \int_{x_1}^{x_2} f_X(x) dx = \lambda \int_{x_1}^{x_2} e^{-\lambda x} dx$$

The cumulative distribution function (CDF) is, in turn, found by integration

$$F_X(x) = P[X \leq x] = \int_0^x f_X(u) du = \int_0^x \lambda e^{-\lambda u} du$$

Table 1a: Summary of gauge depth (d) measurements. For exact boundaries of the various regions see text. Data are tabulated for all water depths and in 5-m water depth classes. The λ values are calculated using $(d - 0.2)$ where 0.2 m defines the origin of the distribution. The $d_{0.2}$ values are calculated using a 0.2 m cutoff while the d values use an extrapolated value (given in parentheses) for the 0.1 m class interval (see text).

Id oint of lass nternal	A. All Water Depths				B. Lagoons & Sounds			C. Lonely					D. Harrison Bay				E. Jones Is. and East					
	ones Is. nd East	Harrison Bay	Lonely	Lagoons and Sounds	0-5 m	5-10 m	10-15 m	0-5 m	5-10 m	10-15 m	15-20 m	20-25 m	0-5 m	5-10 m	10-15 m	15-20 m	5-10 m	10-15 m	15-20 m	20-25 m	25-30 m	30-35 m
.1	(10176)	(14601)	(2595)	(189)	(59)	(289)		(441)	(1750)	(1151)	(917)	(488)		(444)	(759)	(573)	(115)	(497)	(3281)	(6915)	(3390)	(308)
.3	9401	646	1802	36	18	17	1	21	405	975	336	65	22	157	378	89	47	408	1685	4070	2427	764
.5	4023	124	673	4	2	1	1	1	56	387	203	26		16	96	12	6	49	401	1661	1486	520
.7	1378	32	253	1	1				4	156	91	2		5	25	2	4	12	91	426	604	241
.9	957	16	87						3	45	39			2	14		1	2	46	250	482	176
1.1	450	6	32							15	17							2	17	93	252	86
1.3	188		12							5	7							2	4	41	94	47
1.5	135		8							5	3								2	28	72	33
1.7	42		1							1									1	8	23	10
1.9	26		0							0										3	12	11
2.1	9		0							0										3	5	1
2.3	5		1							1											4	1
2.5	2																				1	1
2.7	2																				1	1
2.9	1																				0	1
3.1	0																				0	0
3.3	0																				0	0
3.5	1																				1	1
N	16620	824	2869	41	21	18	2	22	468	1590	696	93	22	180	502	103	58	475	2247	6483	5464	1893
λ	3.47	6.13	4.59	1.74	7.24	9.00	5.00	9.17	7.62	4.51	3.58	6.08	10.0	7.38	5.46	7.631	6.30	7.10	5.76	4.47	2.98	2.7.
$d_{0.2}$.47	.36	.42	.33	.34	.31	.40	.31	.33	.42	.48	.36	.30	.34	.38	.33	.36	.34	.37	.42	.53	.5"
$\frac{d}{r^2}$.33	.19	.27	.14	.16	.11	.30	.11	.15	.29	.26	.14	.20	.17	.21	.10	.19	.22	.21	.26	.37	.31
r^2	.96	.97	.94	.98	.92	1.00	1.00	1.00	.93	.91	1.00	.93	1.00	.95	.96	1.00	.94	.86	.99	.99	.94	.9.

Table 1b: Summary of gouge depth (d) measurements {cont.}. For additional details see table 1a and text.

Midpoint of class interval	All regions (C+D+E) excluding B. Lagoons and Sounds						
	0-5 m	5-10 m	10-15 m	15-20 m	20-25 m	25-30 m	30-35 m
.1	(1849)	(2196)	(1953)	(5273)	(7006)	(3390)	(1460)
.3	43	609	1761	2110	4135	2427	764
.5	1	78	532	616	1587	1486	520
.7		13	196	184	428	604	241
.9		6	61	85	250	482	176
1.1			24	34	93	252	86
1.3			7	11	41	94	47
1.5			5	5	28	72	33
1.7			1	1	8	23	10
1.9			0		3	12	11
2.1			0		3	5	1
2.3			1			4	1
2.5						1	1
2.7						1	1
2.9						0	1
3.1						0	
3.3						0	
3.5						1	
N	44	706	2588	3046	6576	5464	1,893
λ	9.57	7.43	5.03	5.09	4.48	2.98	2.73
$\sigma_{0.2}$.30	.33	.40	.40	.42	.54	.57
\bar{d}	.10	.16	.27	.21	.26	.37	.36
r^2	1.00	.97	.92	.99	.99	.94	.95

$$= -e^{-\lambda x} \Big|_0^x = 1 - e^{-\lambda x} \quad x \geq 0$$

Finally, because we are interested in the probability of occurrence of gouges that have depths greater than or equal to some specified value, we are **largely concerned** with the value of the exceedance probability given by the complementary distribution function $G_X(x)$

$$G_X(x) = P[X \geq x] = 1 - F_X(x) = e^{-\lambda x} \quad (2)$$

$G_X(x)$ is a particularly simple function to graph as **it** is a straight line on semi-log paper and has a **value** of 1 at $x = 0$. Therefore the simple relation

$$P[D \geq d] = \frac{n[D \geq d]}{N} = e^{-\lambda d} \quad (3)$$

can be used to estimate $n[D \geq d]$ (the expected number of gouges having depths greater or equal to d given that N gouges have occurred). Values for λ for the four data sets shown in Figure 7 are given in **Table 1a**. In determining λ the fact that the 0 to 0.2 m gouge depth class was excluded was handled by letting $d' = (d - c)$ where $c = 0.2$ m, the cutoff value. Note that in **Figure 9** the nominal $d = 0$ location is, in fact, $d = 0.2$ m. Note also that when the number of gouges are given, only gouges having depths equal to or greater than 0.2 m are counted. The use of a cutoff has an undesirable effect on the estimates of the mean gouge depth in that the value obtained depends upon the cutoff in use (in **Table 1** the value $\bar{d}_{0.2}$ refers to a mean gouge depth calculated using the 0.2 m cutoff), **To** facilitate comparisons between our data set and those of other investigators we also include \bar{d} values in **Table 1** which are calculated by first estimating the

number of gouges in the 0 to 0.2 m class interval by exponential extrapolation and then including this estimate in the calculation of the mean. The use of the resulting values, of course, implicitly assumes that the distribution of gouge depths is exponential. The values given in () in Tables 1a and 1b for the 0.1 m class interval are the extrapolated values.

It is, however, possible to sharpen up the above by noting that, at least off the Mackenzie Delta, the nature of the gouge depth distribution is known to change with water depth (Lewis, 1977a). We **will** now examine the effect of such a variation within our study area. That similar changes **will** be found to occur in the Alaskan Beaufort can be surmized from Figure 7 in that the shallower areas (lagoons and sounds and Harrison Bay) show no deep gouges. The λ and \bar{d} values corresponding to various 5-m water depth classes in the different regions are given in Table 1a and the λ values are plotted against water depth (z) in Figure 8. There is **clearly** a **general** decrease in λ with increasing z within the range of the data set. For a discussion of the area in general, we have combined all the data for "offshore" areas unprotected by barrier islands (Lonely + Harrison Bay + Jones Islands and East) into one data set (Table 1b). Figure 9 gives 3 representative plots of data from this combined set for three different 5-m water depth intervals and also shows the fitted curves based on equation (1). Figure 10 shows the seven λ **values** for this combined set plotted versus z . We have chosen to fit the λ versus z data with a negative exponential ($r^2 = 0.95$) purely as a matter of convenience. This **curve** **should** not be extrapolated beyond the range of the data. For instance it

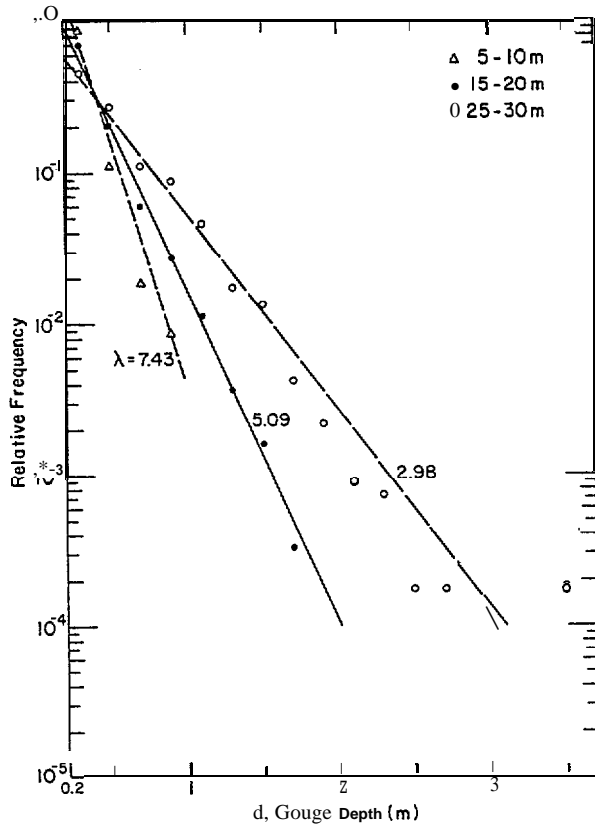


Figure 9. Relative frequency of occurrence of gouges of differing depths based on all data from "offshore" areas unprotected by barrier islands.

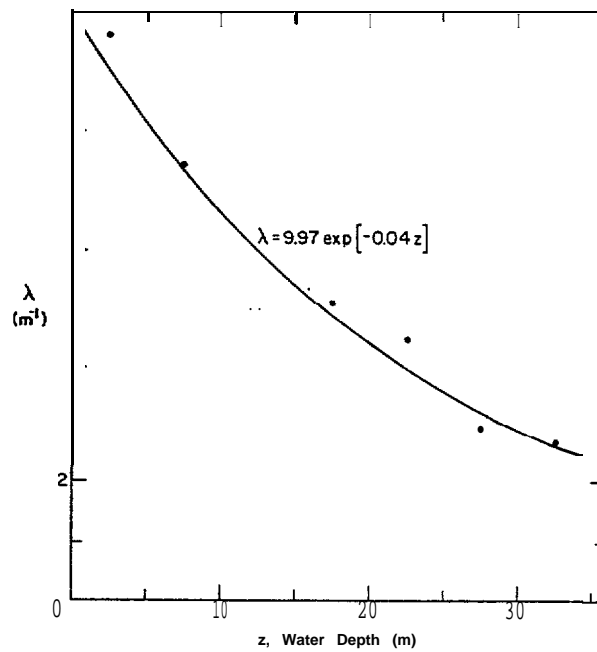


Figure 10. λ values (m^{-1}) versus water depth (m) based on the data set from "offshore" areas unprotected by barrier islands.

is known (Lewis, 1977a) that gouges off the Mackenzie Delta do not appear on the sea floor at water depths greater than 80 m and show a peak in the mean gouge density at a water depth of 23 m. Therefore, one might expect that in the present study area λ values may increase again at $d_w > 35$ m.

Clearly water depth is a most important parameter in studies of gouging.

v* GOUGE-ORIENTATIONS

Determining the absolute cartographic orientation of every gouge would be very time-consuming. To provide some information on gouge orientations we have visually estimated the dominant orientation that exists along each kilometer of sample track. These orientation values do not provide information on the actual direction of the ice movement {for instance, the direction 90° indicates only that the gouge runs along the $90^\circ - 270^\circ$ line (in the E-W direction)}. **Figure 11** shows **linear** histograms of the probability of the occurrence of different orientations. The data are displayed between 0 and 180° . This proved to be convenient as there was a natural break in the observations at this orientation (i.e., very few gouges were aligned N-S). Summary statistics for these observations are presented in Table 2. The mean given here is the **circular** mean as calculated for **axial** data; the circular variance has a **value** near zero if the data are tightly clustered and a value near 1 if the directions are widely dispersed; and the standard deviation is somewhat analogous to the ordinary standard deviation **on** a line (Mardia, 1972, p. 18-27).

Figure 11 and Table 2 show several obvious things. First, the dominant gouge orientations appear to have a **unimodal** distribution that **is**

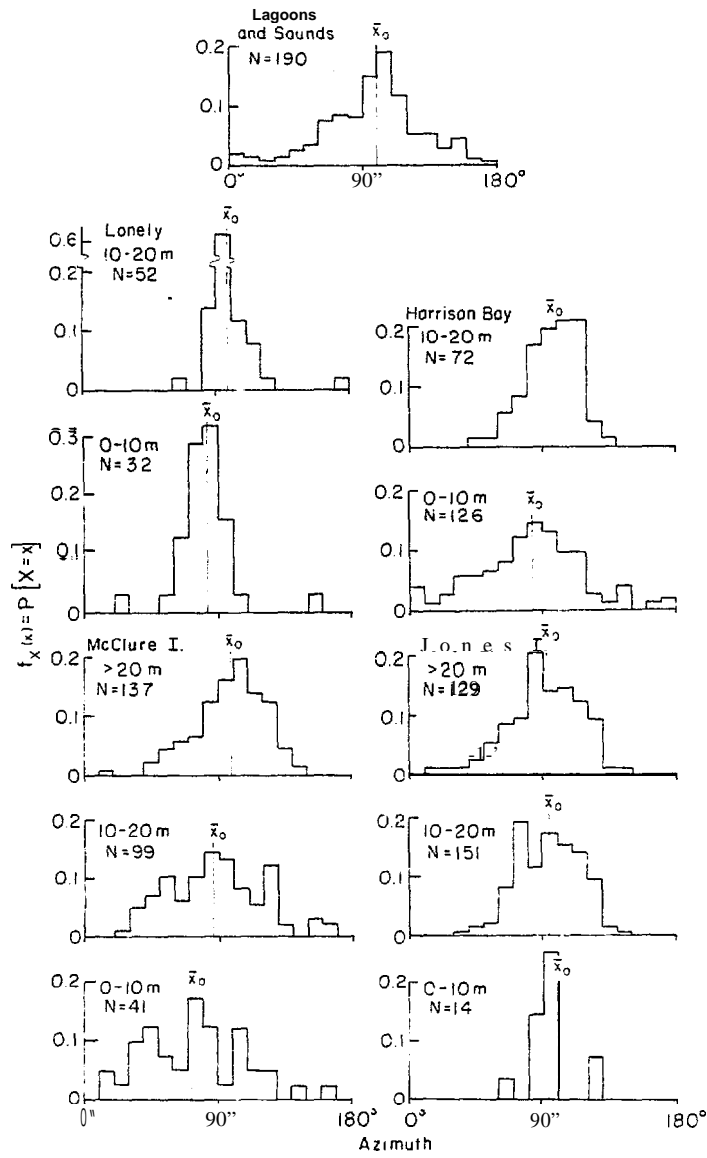


Figure 11. Linear histograms of the observed probability of different dominant gouge orientations.

Table 2. Descriptive statistics on the variations in the dominant orientations of the gouges.

Location	Water Depth Range (m)	Sample Size N	Mean <u>Direction</u> \bar{x}_o (deg.)	Circular Variance so	Standard Deviation s (deg.)
Lagoons and Sounds	all	0190	99.2	.142	15.9
Lonely	o-1o	32	80.3	.045	8.7
	10-20.4	52	96.6	.023	6.2
Harrison Bay	0-10	126	82.7	.162	17.0
	10-20	72	97.4	.047	8.9
Jones Island	o-1o	14	93.8	.032	7.4
	10-20	151	94.0	.066	10.6
	>20	129	92.3	.081	11.8
McClure Islands	o-1o	41	71.6	.169	17.4
	10-20	99	86.4	.149	16.3
	>20	137	99.0	.080	11.7

reasonably clustered. Second, gouge orientations show more variability in the lagoons and sounds and in other shallow water (0-10 m) areas. Farther off the coast in deeper water, these variations generally decrease (increased clustering; lower S_0 and s values). The average orientation in water >20 m deep is 97 to **99°T**, which is just a few degrees less than parallel to the coast (110°T). In shallow areas the gouges generally show a higher angle (71 to 83°T) to the coast although this tendency is not evident in the measurements made off the Jones Islands, **It** is reasonable to expect a floe that is in process of grounding to rotate and move toward the coast (this effect has been observed in radar imagery at Barrow by Shapiro (**pers.** communication). However, it is not **clear** to us why this phenomena should be more pronounced in shallow water. The mean orientations for gouges located in deeper water are similar to orientations (101 to 103°T) observed at the same water depths off the Mackenzie Delta (Lewis, 1977a). However, there was no apparent decrease in gouge azimuth in the shallow water locations at the Canadian **site**.

The main factor in controlling the orientation of the gouges is presumably the wind direction, which at **Kaktovik** is predominantly in two directions: from the **ENE-E** (55-100°T) 35% of the time and **WSW-W** (235-280°T) 23% of the time. The mean wind speed is the same (6.7 m/s) in both directions (**AP0, 1978**). These directions are in excellent correspondence with the observed gouge orientations.

The mean gouge orientation in the lagoons is 99°T which is similar to the gouge orientations in water deeper than 20 m. As the direction of elongation of the lagoons and sounds is roughly 105°T, the mean gouge

orientation occurs between the orientation of the container (the lagoon) and **the** orientation of the forcing function (the wind).

VI. GOUGE FREQUENCY

We now have a reasonable description of the probability of a gouge having different gouge depths given that a gouge has occurred. Next we need to determine how many gouges have occurred so that we can estimate N in equation (2). The number of gouges that is of primary interest is the temporal gouge frequency (the number of gouges that intersect a unit length of line per unit of time (e.g. gouges per kilometer per year). As will be seen, data leading to such estimates are extremely sparse. What is available are measurements of the spatial gouge frequency (e.g. gouges per kilometer) as seen at a given location at essentially a fixed instance in time. We will now discuss these two parameters.

A. Spatial Gouge Frequency

To study variations in the spatial gouge frequency **the** number of gouges deeper than 0.2 m per kilometer was determined for each kilometer of sampling track. These values were then converted to N_1 , the number of gouges per kilometer that would have been encountered if the sampling track was **oriented** perpendicular to the trend of the gouges. The **values** were then separated into 5 different groups (lagoons and sounds, Lonely, Harrison Bay, Jones Islands, and McClure Islands and East) and **plots** were made of N_1 versus water depth. Examination of these **plots** showed that lagoons and sounds were different from the other four areas in that gouging was rare (92% of the 298 kilometers sampled contained no gouges and the largest N_1 value was 12 gouges/km). The four other regions showed dif-

ferences **but** these appeared to **be** largely caused **by** changes in **the** water depths sampled in the different areas. Therefore all four regions were combined and considered as one. Figure 12 shows the N_1 versus z plot for the combined data. A data tabulation is presented in Table 3. As was the case in the lagoons, in shallow water N_1 values of zero (N. values) are common and N_1 values greater than 50 are rare. In water 15 to 20 m deep, zero values become less common and larger N_1 values are encountered. Finally as water depths increase above 22 m, all samples show 20 or more gouges per kilometer. These changes can be shown (Figure 13) by taking 10 m wide vertical slices through Figure 12 and displaying the results as histograms giving relative frequency versus $(N_1/10)$. As can be seen, in the lagoons **and** sounds there is a rapid exponential drop-off in frequency as the $(N_1/10)$ value increases. In shallow water (<10 m) outside of the barrier islands the trend is similar although null values are not as frequent (42%). At depths of 10 to 20 m the **null** values compose only 24% of the **total sample** and $(N_1/10)$ values in excess of 10 are not rare. In deeper water the distribution from 20 to 30 m and 30 to 38 m had nearly identical means and forms and were therefore combined. The histogram is now more nearly Gaussian and shows only a **slight** positive skew. Again **clearly** the nature of the distribution is a function of the water depth. One additional piece of information should be added here. At one location (off of Lonely) a study was made of the distribution of the spacings between gouges (as measured along the sampling line). Again the distribution was a negative exponential (Figure 14).

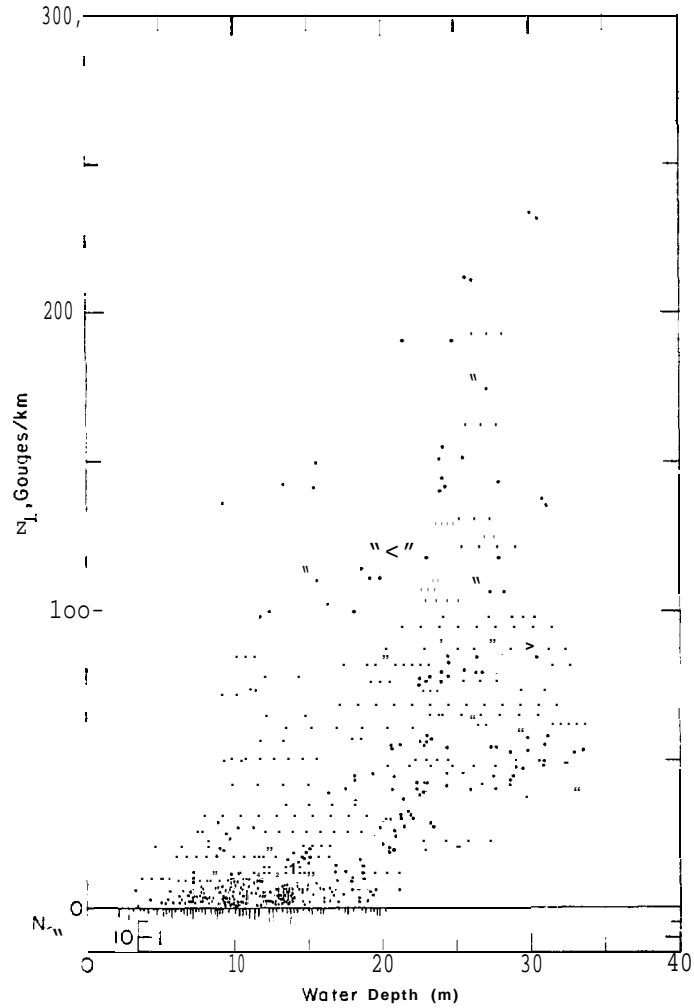


Figure 12. Number of gouges per kilometer measured normal to the trend of the gouges (N_1) versus water depth (m).

Table 3. Summary of the observations on the number of gouges deeper than 0.2 m per kilometer.

N _i number of gouges deeper than 0.2 m per kilometer	Frequency of occurrence (Lagoons and sounds)	(N _i /10) number of gouges deeper than 0.2 m per 100 m	Frequency of Occurrence Offshore (all sites except lagoons and sounds)		
			0-10 m	10-20 m	20-38 m
			0	275	0
1	7	1	67	154	5
2	8	2	10	31	13
3	4	3	5	20	15
4	0	4	2	12	19
5	2	5	2	12	27
6	1	6	1	9	21
12	1	7	2	7	23
N = 298		8		10	26
		9		4	16
		10		4	21
		11		5	8
		12		5	9
		13		0	9
		14		2	7
		15		0	4
		16		1	3
		17		0	1
		18		0	2
		19		0	5
		20		0	3
		21		0	0
		22		1	0
		23			2
		24			0
		25			0
		26			0
		27			1
N =			151	365	242

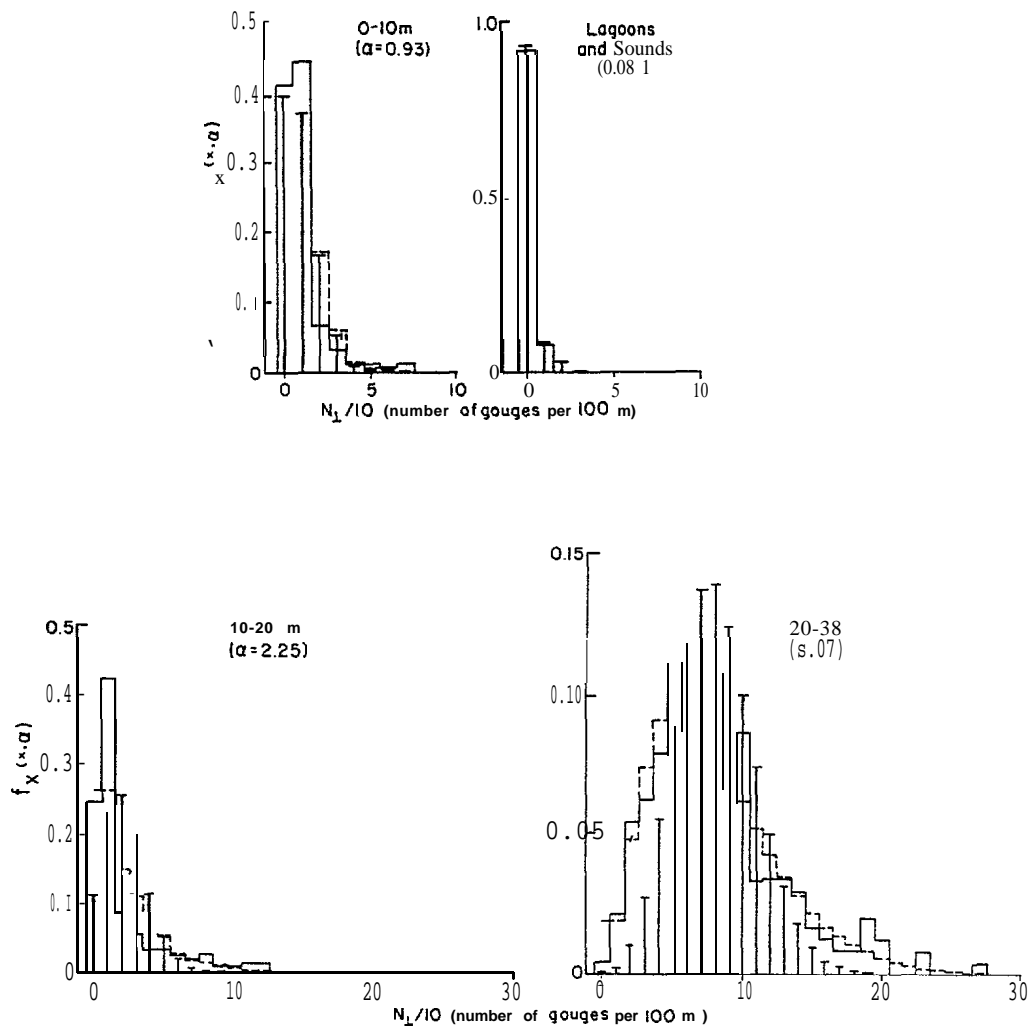


Figure 13. Relative frequency of different values of $N_1/10$ for lagoons and sounds and 3 different water depths offshore of the barrier islands.

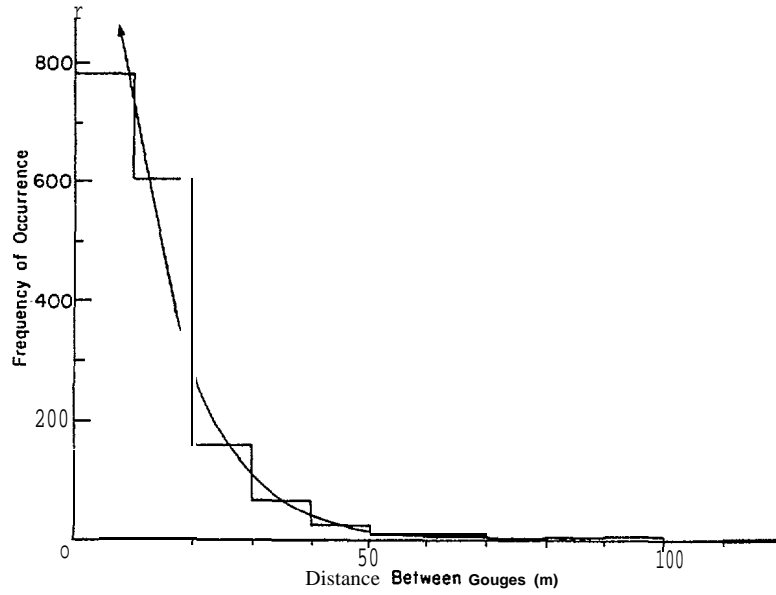


Figure 14. Frequency of occurrence versus the observed distances between the gouges off Lonely, Alaska.

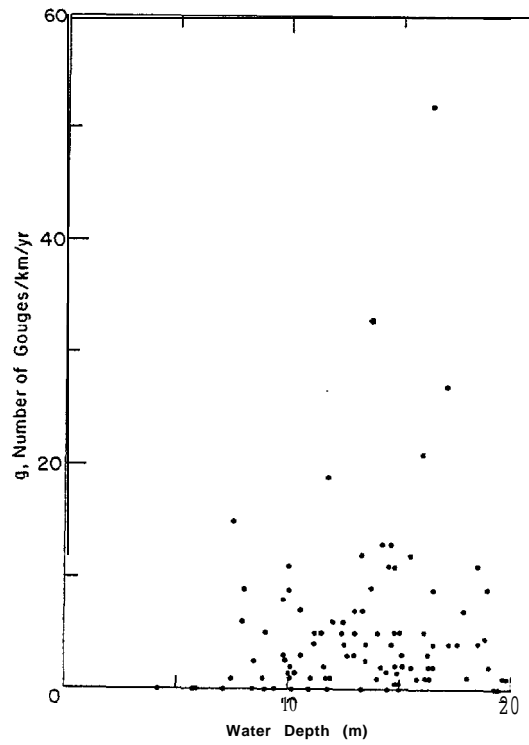


Figure 15. Number of gouges/km/yr (g) versus water depth (m).

It **would** be convenient to have one distribution function that would describe all the histograms shown in figure 13. If possible this distribution should have the following characteristics:

- (a) it should be discrete in that we are describing a counting process (either a gouge is present or it is not),
- (b) it should be capable of dealing with the finite occurrence of zero values,
- (c) it should have a shape which varies from a negative exponential to normal as the mean value of N_1 increases, and
- (d) the distribution of spacings between occurrences should be given by the exponential distribution.

The Poisson distribution has, in fact, all these characteristics and is given by

$$f_x(x, \alpha) = \frac{\alpha^x e^{-\alpha}}{x!}, \quad x = 0, 1, 2, 3 \dots \alpha > 0 \quad (4)$$

where the parameter α is the sample mean which in our case varies from 0.08 for lagoons and sounds to 8.07 for depths in excess of 20 m. As we have plotted $(N_1/10)$, these sample means correspond to N_1 values of 0.8 and 80.7 gouges/km. The use of $(N_1/10)$ was necessitated by the fact that N_1 values as large as 270 gouges/km occur. The Poisson distribution, on the other hand, is not convenient for values much in excess of 20. When $(N_1/10)$ is used, the Poisson probability for an integer such as 3 is used to represent the probability of N_1 occurring in the interval $25 \leq N_1 \leq 35$ gouges per kilometer. Examination of Figure 13 shows that the Poisson distribution does, in fact, give a reasonable representation of the frequency plots of

the N_1 values although **it** does appear to drop **off** too rapidly at large ($N_1/10$) values. The Poisson distribution also possesses the additive property that the sum of two Poisson random variables with parameters α_1 and α_2 is also a Poisson random variable with parameter $\alpha = \alpha_1 + \alpha_2$.

The use of the Poisson distribution brings to mind its association with the Poisson process describing the occurrence of random events occurring at a constant rate **along** a continuous space (or time) scale. To be a Poisson process the underlying physical mechanism generating the events must satisfy the following three assumptions

- 1) **Stationarity** - the probability of an event in any short interval **is** proportional to the length of the interval.
- 2) **Nonmultiplicity** - the probability of two or more events in a short interval Δx is negligible in **comprison** to $\alpha \Delta x$.
- 3) **Independence** - the number of events in any interval is independent of the number, of events in any non-overlapping interval.

The probability distribution of the number of events N in distance x for a **Poisson** process is given by

$$f_N(n; vx) = \frac{(vx)^n e^{-vx}}{n!}, \quad n = 0, 1, 2, 3, \dots; vx > 0 \quad (5)$$

where vx has replaced α in equation (4) and the parameter v is the average spatial rate of occurrence of the event.

We would judge **that,when** gouging is looked on as an annual event, it **would** satisfy the requirements for a Poisson process reasonably well as a first approximation. We however note that when the spatial distribution of

gouging is examined in more detail it is found that there are locations where gouges occur in groups (on the seaward sides of shoals). Also gouges presumably are more common in areas where the surface sediments are poorly bonded than they are in regions where the surface sediments show a high strength. In addition if gouging is examined on a time scale finer than yearly, the assumption of **stationarity** is clearly not satisfied as in many locations no gouging occurs during the summer months, However these **problems** are probably no worse than in many other areas such as customer arrivals and number of telephone calls per unit time where the Poisson process has been found to be a very useful model.

It is, of course, possible to use other distribution functions such as a gamma distribution. This distribution is attractive for several reasons. First **it is** capable of assuming shapes similar to those shown in Figure 13 (Hahn and Shapiro, 1967, Figures 3-7b and 3-8). It is also an applicable distribution to data such as N_1 that are bounded on one end (however it is not capable of treating the occurrence of zero values). In addition this distribution has been used successfully in a variety of engineering problems because of its flexibility (Benjamin and Cornell, 1970). The gamma distribution is given by

$$f_X(x) = \frac{\lambda^\eta x^{\eta-1} e^{-\lambda x}}{\Gamma(\eta)} \quad x \geq 0, \lambda > 0, \eta > 0 \quad (6)$$

where $\Gamma(\eta)$ is the gamma function

$$\Gamma(\eta) = \int_0^\infty x^{\eta-1} e^{-x} dx \quad (7)$$

Here **the** two free parameters η and λ can be considered **to** be shape **and** scale parameters respectively. The mean, variance and coefficient of skew for the distribution are respectively

$$E(x) = \eta/\lambda \quad (8)$$

$$\text{Var}(x) = \eta/\lambda^2 \quad (9)$$

$$Y = 2 \sqrt{\eta} \quad (10)$$

The exponential distribution is, in fact, a special case of the gamma distribution with $v = 1$.

As can be seen in Figure 13 the gamma distribution gives a very **reasonable** representation of N_1 data if the presence of zero values is arbitrarily introduced in calculating the appropriate probabilities. Note that the gamma distribution **is** more successful in fitting the **larger** ($N_1/10$) values **than is** the Poisson distribution which drops off too quickly at large values of ($N_1/10$). **Table** 4 gives the values of the parameters of the fitted gamma distributions. The λ and η values were obtained using the maximum likelihood procedure suggested by Thorn (see Haan, 1977, p. 102-6). In comparing the Poisson and the Gamma mean values it **should** be remembered that the Poisson mean includes the effects of **the** presence of zero N_1 values while the gamma mean does not.

B. Temporal Gouge Frequency

In investigating problems concerning ice induced gouging of the sea-floor it is highly desirable to have independent information on the rates at which new gouges form (the number of new gouges per kilometer per year). Unfortunately such data are rather limited, and for our **studyarea**

Table 4. Parameters of gamma distributions fitted to observational **data** on the number of gouges/kilometer (N_{\perp}) for lagoons and sounds and to observational data expressed in terms of **the** number of gouges/100 m ($N_{\perp}/10$) for the combined offshore data set.

Region	Depth Interval	Number of kilometers sampled	Number of kilometers with gouges	Data units	Shape Parameter η	Scale Parameter λ	Mean (Ii/A)	Variance (η/λ^2)	Coef. of_skew ($2/\sqrt{\eta}$)
Lagoons & Sounds	All depths	298	23	gouges per km	2.155	0.787	2.738	3.479	1.362
Combined Offshore Data Set	0-10 m	151	89	gouges per 100 m	2.899	1.842	1.574	0.854	1.175
	10-20 m	365	277	gouges per 100 m	1.296	0.436	2.972	6.818	1.757
	20-38 m	242	241	gouges per 100 m	3.023	0.373	8.105	21.729	1.150

are largely contained in a paper **by** Barnes et al. (1978). This work describes replicate observations made on sample line 35 (see Figure 5 for location) during **the** summers of 1973, 1975, 1976, and 1977 and on line 31 made during the summers of 1975, 1976 and 1977. We have reanalyzed the data set from line 31 for the 1976-77 year and on line 35 for the 1976-77 and 1977-78 intervals so that the counts of new gouges are based on 1-km sampling lines. We have also analyzed replicate runs on line 39 (north of Cape **Halkett**) for 1977-78.

Because the quality of the 1973 sonar records were poor (**Reimnitz et al.**, 1977a), the data based on the 1973-75 time interval **should** receive less weight than the later observations. The results of this analysis plus that of Barnes et al. (1978) are combined and presented in Table 5. We have arbitrarily deleted the \bar{g} values obtained on line 39 at 20.3 m and further offshore in that this portion of the line is known to be in **the** shadow of a nearby shoal area thereby receiving less gouges. If the 1973-5 data on test line #35 is also excluded because of the poor quality of the sonar record we obtain an average \bar{g} value of 5.2 gouges per kilometer per year with values for individual years varying from 2.4 (1975-6) to 3.5 (1976-7) to 7.9 (1977-8). These are appreciably **larger** values than have been obtained using similar procedures off the Mackenzie Delta in 15 to 20 m of water (0.19 ± 0.06 gouges per kilometer per year, Lewis 1977a) giving a return period per kilometer of 0.2 years as compared to 5.3 years.

Figure 15 shows a plot of observed g values versus water depth. There is no strong trend. In addition there is a **large** scatter and zero values (1 km lines with no new gouges) are rather **evenly** distributed at all water

Table 5. Number of new gouges during the indicated time and space intervals as determined from replicate sonar data collected during the summers of the years indicated. The 1973-5 and 1975-6 data are from Barnes et al. (1978). The symbol - indicates no data was collected. Also given are values of \bar{g} , the average number of new gouges per kilometer per year.

Interval on line (km)	Test Line #35					Line #31			Line #39	
	\bar{d}_w (m)	1973 to 1975	1975 to 1976	1976 to 1977	1977 to 1978	\bar{d}_w (m)	1975 to 1976	1976 to 1977	\bar{d}_w (m)	1977 to 1978
0-1	5.9	—	--	--	0	8.9		1	4.2	0
1-2	7.5	—	--	1	15	11.0	3	1	5.8	0
2-3	8.0			6	9	11.7		1	7.1	0
3-4	9.0	2	5	5	0	12.0	2	6	8.4	0
4-5	9.8			8	3	13.0		5	9.4	0
5-6	0.0	4.5	5	11	9	14.0	5	1	0.2	0
6-7	0.1			2	1	14.8		5	0.9	0
7-8	0.6	0	3	7	3	15.0	3	5	1.6	2
8-9	.1.2			5	4	14.6		4	2.4	5
9-10	1.8	1	10	0	19	15.1	1	2	3.3	0
10-11	2s5			6	4	15.8		1	4.0	5
11-12	3.0	.5	6	7	3	16.3	10	2	4.6	13
12-13	3.3			7	12	17.2		4	5.0	0
13-14	3.7	1	8	9	33	18.0	8	1	5.5	12
14-15	4.2			2	13	18.5		4	6.3	52
15-16	4.5	1.5	3	0	11	19.0	9	2	7.1	27
16-17	4.8			2	11	19.4		0	7.9	7
17-18	5.1		1	3		19.8		1	8.5	11
18-19	5.4			—	--	20.3		1	8.9	9
19-20	5.6		4	--	--				9.3	0
20-21	5.8			--	--				9.7	1
21-22	6.0			—	21				0.1	6
22-23	6.3			1	3				0.3	0
23-24	6.5		6	4	9				0.4	0
24-25	6.5			2					0.2	0
25-26									9.2	0
26-27									7.9	2
27-28									7.3	0
28-29										0
\bar{g}		0.4	2.1	4.4	9.2		1.1	2.5		6.8

depths . Because of this we have treated all the observations as a **single** group. Figure 16 shows a plot of the observed probability of occurrence of different values of \bar{g} . The distribution shows a strong positive skew. The Poisson distribution for this set of data is also shown. The representation of the data is not encouraging (again the probability of occurrence falls off much too rapidly at large g values). Also shown is a gamma distribution which gives a better fit (the shape and scale parameters are respectively $\eta =$ and $\lambda =$)*

While the characteristics of the new gouges are being discussed, it is of interest to examine the distribution of their depths to see if it appears to **follow** an exponential distribution similar to that obtained by sampling **all** the gouges on the seafloor, a data set which of course contains a number of old gouges that presumably have been partially filled with sediment as **well** as new unfilled gouges. The observations used ($n = 76$) were from both test lines 31 and 35 and occurred between 1976 and 1977. The results are shown in **Figure 17**. Again the data appears to show an exponential dropoff with a λ value of 4.52 m^{-1} . This value is close to but somewhat lower than the **values** obtained from the samples of all the gouges (taking 15 m as a mean water depth **along** the replicate sampling lines, we obtain a value of 5.5 m^{-1} from Figure 10 as contrasted with 4.5 m^{-1} from the new gouges). That new gouges should have a lower λ value than a corresponding distribution of old and new gouges could be anticipated (E. **Phifer**, pers. com.) from the observation that at other locations deep gouges in the seafloor receive more fill per year than do shallow gouges (**Fredsoe** 1979). At the present there clearly is no strong reason to doubt

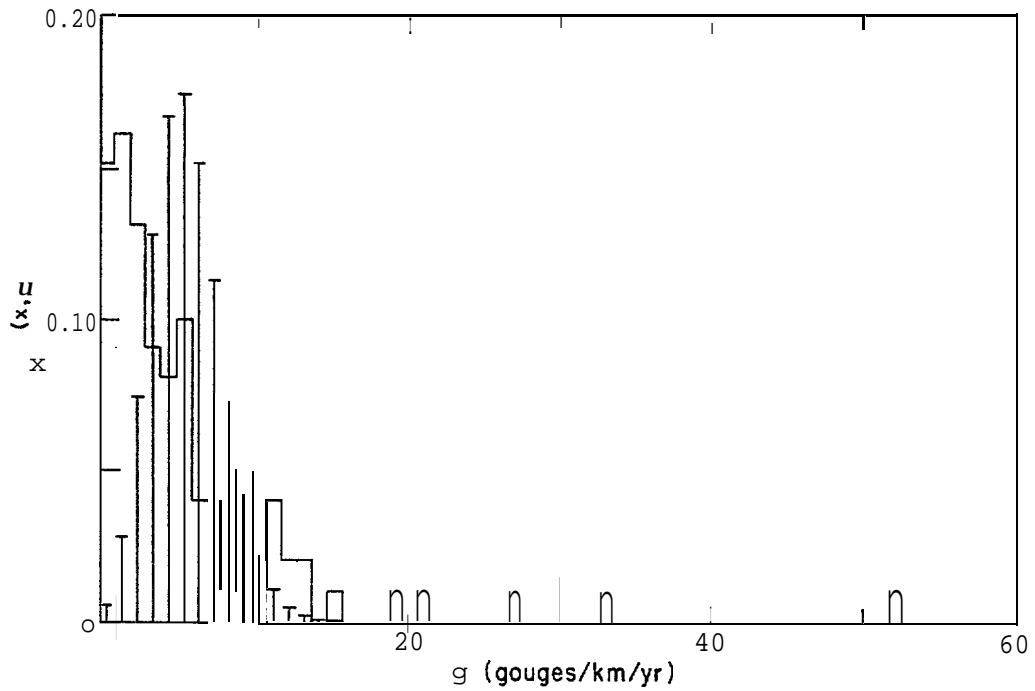


Figure 16. Relative frequency of different values of g (number of gouges/km/yr) . The discrete distribution is a fitted Poisson and the stippled distribution is a fitted Gamma.

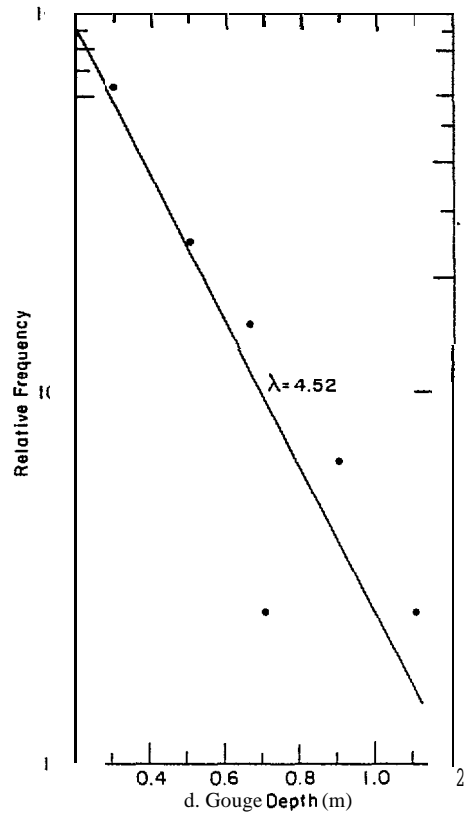


Figure 17. Semi-log plot of the relative frequency of occurrence of new gouges of differing depths (m).

that the distribution of new gouge depths is exponential or that the λ values that will be obtained are greatly different (presumably slightly **less**) than **values** obtained from our earlier analysis of **all** the gouges.

VII . EXTREME VALUE ANALYSIS

Another way to view portions **of** the gouging data is by extreme value analysis. **In** this case the complete data set is not examined. Instead the largest (or smallest) value in each of a number of specified sampling intervals was used. In most applications, such as **in** hydrology, the data are in the form of time series and the largest (smallest) event in each of a sequence of fixed time intervals is used to generate a distribution of rare events. **In** our study, the basic data set is a space-series as separate frequency distributions of gouge characteristics were developed for each kilometer of sampling **line**. For instance, in a kilometer of line one might observe 85 gouges of different depth, with the largest gouge having a **value** of 2.2 m; in the next kilometer there might be 178 gouges with a maximum value of 3.1 m. The extreme value distribution **would** then be composed of the values 2.2, 3.1 and subsequent values. Good discussions of the different types of extreme value distributions can be found in Hahn and Shapiro (1968), Benjamin and Cornell (1970) and Haan (1977).

The particular extreme value distribution applicable to a given situation depends on the **nature** of the initial distribution being sampled and on **the** sample size n , with the extreme distribution being approached asymptotically as n becomes large. A common problem is that many **times** n does not appear to have been large enough, and the extreme value distribution that would be expected to apply to a given data set is **not particu-**

larly successful in fitting it. For instance, a Type I extreme value distribution should apply to maximum values sampled from an initial distribution that is of the exponential type. However Tucker et al. (1979), in their study of maximum pressure ridge heights, whose initial distribution appears to be the exponential type, found that their data were not linear on Type I paper but were effectively linearized by standard probability paper. Similar results have been obtained by other workers in hydrology and by Monte Carlo simulations by Slack et al. (1975). In practice, a number of different approaches (Type I, normal, log-normal, log Pearson Type III) are commonly tested and the most successful relation is selected to analyze the data.

A. Gouge Depths

As we have shown, gouge depths appear to be exponentially distributed. Therefore, the appropriate extreme value distribution for maximum gouge depths should be a Type I distribution. However, testing shows that the data were not linearized by either a Type I, a normal or a log-normal distribution. However, a log-Pearson Type III (LPIII) distribution proved to be quite effective. This distribution, which is in fact a three-parameter gamma distribution fitted to the \log_{10} of the extreme values, has been used successfully in treating flood observations (USWRC, 1977). The three parameters describing a LPIII distribution are the mean \bar{X} , the standard deviation S and the skew coefficient G which, if $X \cong \log_{10} d_{\max}$ where d_{\max} is the maximum gouge depth in a kilometer track and N is the number of maximum gouges, are calculated as follows

$$\bar{X} = \frac{\sum x}{N}$$

$$s^2 = \frac{\sum (X - \bar{X})^2}{N-1}$$

$$G = \frac{N \sum (X - \bar{X})^3}{(N-1)(N-2)S^3}$$

The computed d_{\max} value is then given by the relation

$$\log_{10} d_{\max} = \bar{X} + KS \quad (11)$$

where K is the Pearson Type III coordinate expressed in magnitudes of the standard deviation from the mean for various exceedance percentages. Values of K are functions of G and are given in Appendix 3 in USWRC (1977) as are the computing equations for \bar{X} , S, and G.

In analyzing the d_{\max} values on gouging, individual plots (Figure 18) were prepared showing d_{\max} versus d_w for five different areas. Comparisons were made between the different regions by overlaying the figures on top of a light table. If differences in water depth are taken into consideration, the data from Lonely, Harrison Bay, Jones Islands and McClure Islands overlap very well and appear to form one continuous distribution. Therefore, as before the data were pooled into one sample. The data from the lagoons and sounds were treated separately, because they both appear different and represent a different marine environment.

Another characteristic of the d_{\max} data that might be anticipated from our earlier discussion and is apparent in Figure 18 is that the values clearly change with water depth. There are null values, many small values

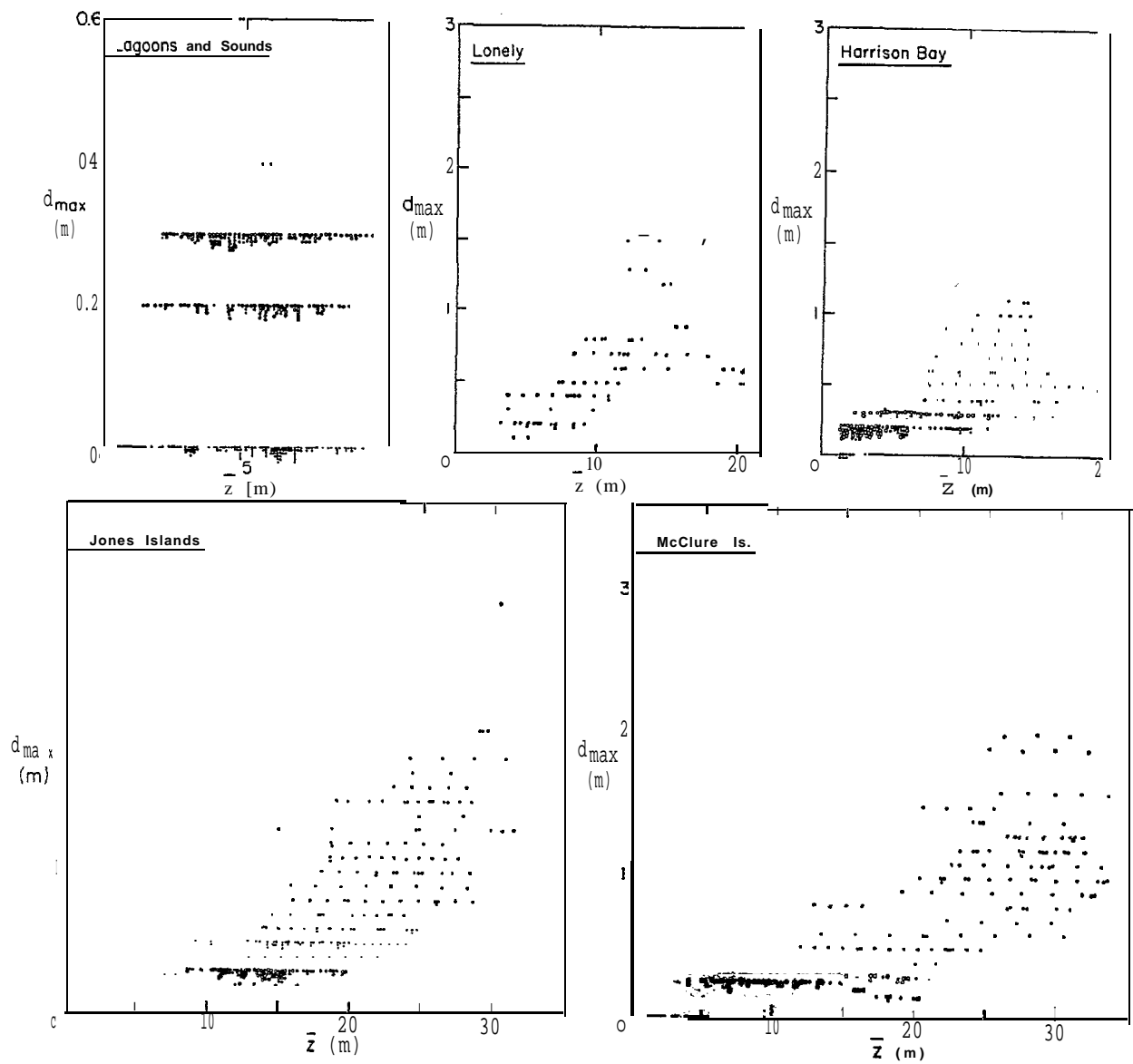


Figure 18. Plots of d_{max} versus water depth (\bar{z}) for 5 different regions within the study area.

and no larger values in shallow water; large values of d_{\max} become increasingly common with increasing d_w ; and small values are rare in water deeper than 20 m. Therefore, as before the pooled offshore d_{\max} data were separated into 5-m water depth increments. As no similar d_w trend was apparent in the data from lagoons and sounds and as the depth range was limited, these results were not separated into similar groups.

In analyzing the data two problems were encountered. First, in a number of shallow water areas we commonly found appreciable lengths of track that did not contain gouges resulting in $d_{\max} = 0$ values. For instance, in the data set for lagoons and sounds, 119 km of the 324 km sampled (37%) were gouge-free. This precludes the normal statistical analysis of the data using a LPIII distribution, as the \log_{10} of zero is minus infinity. Also, in a number of cases it was impossible to precisely determine the depth of the smaller gouges, only that a gouge existed and that its depth was less than some specified value. Some gouge depths are identified by circles in Figure 18. In most cases they had values of less than 0.3 m and were situated in shallow water. This created considerable uncertainty in specifying the exact number of gouges in the 0.1 and 0.2 m depth classes. Where such gouges were common (at water depths of less than 10 in), large G values and LPIII distributions were obtained that were not particularly good fits to the data at the larger d_{\max} values (which, of course, is the area of prime interest).

Both of these problems were handled using a procedure developed for treating zero flood years and incomplete records in hydrology. First, the 0-, 0.1- and 0.2-m values were deleted from the samples. Then the X, S and

G parameters were calculated from the censored distributions and used to calculate d_{\max} as a function of exceedance probability. These **exceedance** probabilities were then adjusted by multiplying them by the ratio of the number of values in the censored distribution to the number of **values** in the uncensored distribution (**i.e.** with the 0, 0.1, and 0.2 values **includ-**ed). The results were then plotted on log-probability paper for comparisons with the observed data. In plotting the data against the adjusted curve, the plotting positions were determined by using the **Weibull** plotting formula

$$P = \frac{m}{N + 1}$$

where P is the exceedance probability, m the sequence of d_{\max} values with the largest values corresponding to $m = 1$, the next largest value corresponding to $m = 2$, etc., and N the total number of data points before censoring (i.e. including 0, 0.1, and 0.2 values).

Table 6 gives the \bar{X} , S, and G values calculated from the different sets of censored data as well as the adjustment **ratio** and the number of d_{\max} values equal to zero and between 0.3 and zero. The exceedance probabilities - the probabilities that given a single kilometer of sample track, the maximum gouge depth will be equal or greater than some indicated value, d_{\max} , are shown in Figure 19. **Also** shown is the spatial recurrence interval for 1 kilometer segments with one or more **exceedances**, which **is** equal to the reciprocal of the exceedance probability. This parameter gives the expected number of kilometers of sea floor that must be observed before the maximum gouge depth in one of those kilometers is expected to

Table 6. parameters of the log Pearson type III distribution determined from values of d_{max} (the maximum gouge depth observed along 1-km sampling lines). The values "outside the barrier islands" include data from Harrison Bay and from north of Lonely.

Location	No. of Values			No. of km of Sample Line	Largest d_{max} Value	$\log d_{max} = \bar{X}$	Standard deviation s	Skew coefficient G	Adjustment Ratio A
	$d_{max} > 0.3$	$0.3 > d_{max} > 0$	$d_{max} = 0$						
Lagoons and sounds	13	192	119	324	0.6	-0.4232	0.1231	0.6909	0.040
Outside the Barrier Is. Depth (m)									
0-5	3	65	11	79	0.4	-0.4812	0.0721	1.7305	0.038
5-10	54	88	0	142	1.1	-0.3466	0.1609	0.5508	0.380
10-15	146	69	0	215	2.2	-0.2623	0.2091	0.4141	0.679
15-20	104	38	0	142	1.7	-0.2282	0.2070	0.3345	0.732
20-25	128	3	0	131	2.1	-0.0933	0.1942	0.0908	0.977
25-30	81	0	0	81	3.6	+0.1095	0.1502	0.3236	1.0
30-35	35	0	0	35	2.9	+0.0964	0.1466	0.4277	1.0

equal or exceed d_{\max} . Another parameter of possible interest is the number of kilometers, per 100 km of sample track, in which the maximum gouge depth is expected to equal or exceed d_{\max} . This number can be obtained by simply multiplying the appropriate exceedance probability by 100. The curves sweep across the graph and show systematic changes with water depth as was expected. The 10 to 15 and the 20 to 25 m curves, which are not shown in order to restrict clutter, lie as expected on the figure. The 30-35 m curve is very similar to the 25-30 m curve, which is not too surprising as there are not many d_{\max} values in the 30 to 35 m range. Also it should be noted that in the plots of d_{\max} vs z from the Mackenzie Delta region (Lewis, 1977a), the d_{\max} values peak out at approximately 40 m and decrease in deeper water.

In Figure 19 the 0-5 m data and the data from the lagoons and sounds overlap each other. As there are only three data points in the 0-5 m data set (as the result of censoring the lower values), the calculated curve was not particularly similar to the curves from deeper water. The curve presented in Figure 19 is based on the data from lagoons and sounds and appears to give a reasonable representation of the 0-5 m data points as well.

Figure 20 presents $\bar{X} = \overline{\log d_{\max}}$, A, G, and S plotted as a function of d_w . This plot should be useful to those interested in developing eq (11) to apply to other water depth intervals than those considered here. The most systematic change in a parameter with d_w is the roughly linear increase in X.

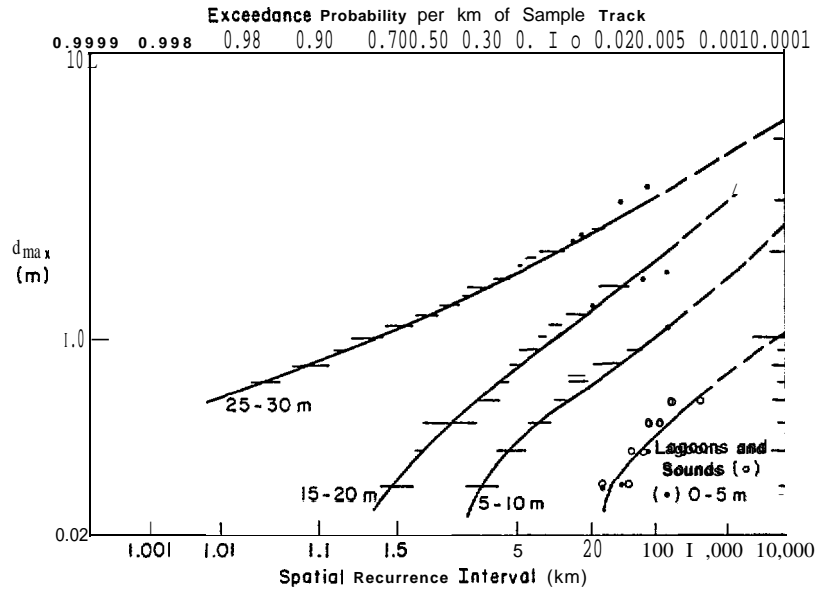


Figure 19. Exceedance probability per km of sample track for different water depths versus d_{max} . The horizontal lines represent the locations of a number of data points (as the data were grouped in class intervals there commonly are several values of the exceedance probability with the same d_{max} (the midpoint of the class interval) value).

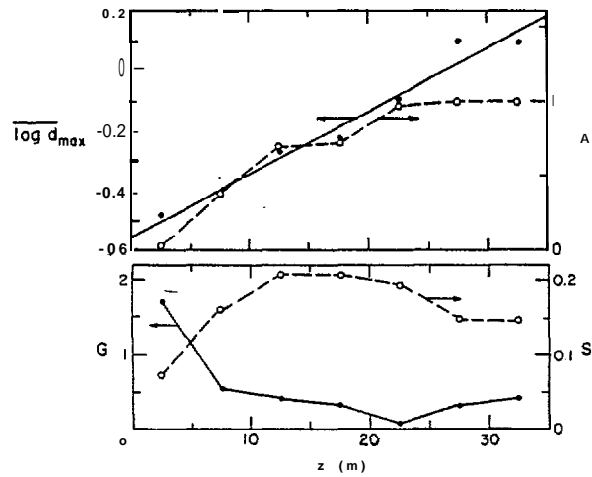


Figure 20. Parameters relating to the determination of eq. (11) shown as a function of water depth (\bar{z}).

B. Gouge Widths

Figure 21 shows all maximum gouge widths (w_{\max}) measured outside the barrier islands compared with the average water depth. The trends are similar to those present in Figure 18, which plotted d_{\max} versus average water depth. There is a general increase in w_{\max} as \bar{z} increases. This may **simply** reflect **that**, on the **whole**, gouges that are deeper are also wider. Also in deeper water there do not appear to be any small w_{\max} values as there were in shallow water.

c. Lateral Embankment Heights

Finally, a comparison of h_{\max} , the maximum lateral embankment height, and d_{\max} is presented in Figure 22 (the numbers indicate the number of values). It is hardly surprising that, on the average, regions with deeper gouges should contain higher embankments as the material from **the** gouges produces the embankments. However, we were surprised at how symmetrically the values were distributed around the 1 to 1 line. This **is** shown by the histogram (see the inset in Figure 22) of the relative frequency of deviations from the 1 to 1 line (measured **normal** to that line).

VIII. APPLICATIONS TO OFFSHORE DESIGN

In the preceding sections we have attempted to systematize and **hope-fully** clarify some of the essential characteristics of a **large** set of measurements on the geometry of ice-induced **gouges** in the sediments of the Alaskan portion of the **shelf** of the Beaufort Sea. These observations are, of course, extremely valuable in themselves. For instance it is very useful to know that outside of the barrier islands in water 38 m or less deep the deepest gouge observed was 3.6 m obtained from a sample of 20,313

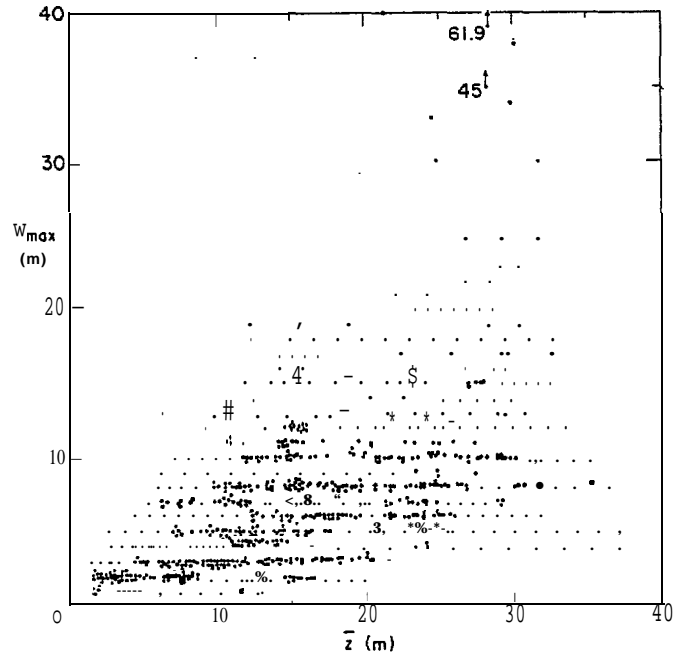


Figure 21. Plot of w_{max} for 1 km line segments versus water depth (\bar{z}) for all locations except those from lagoons and sounds.

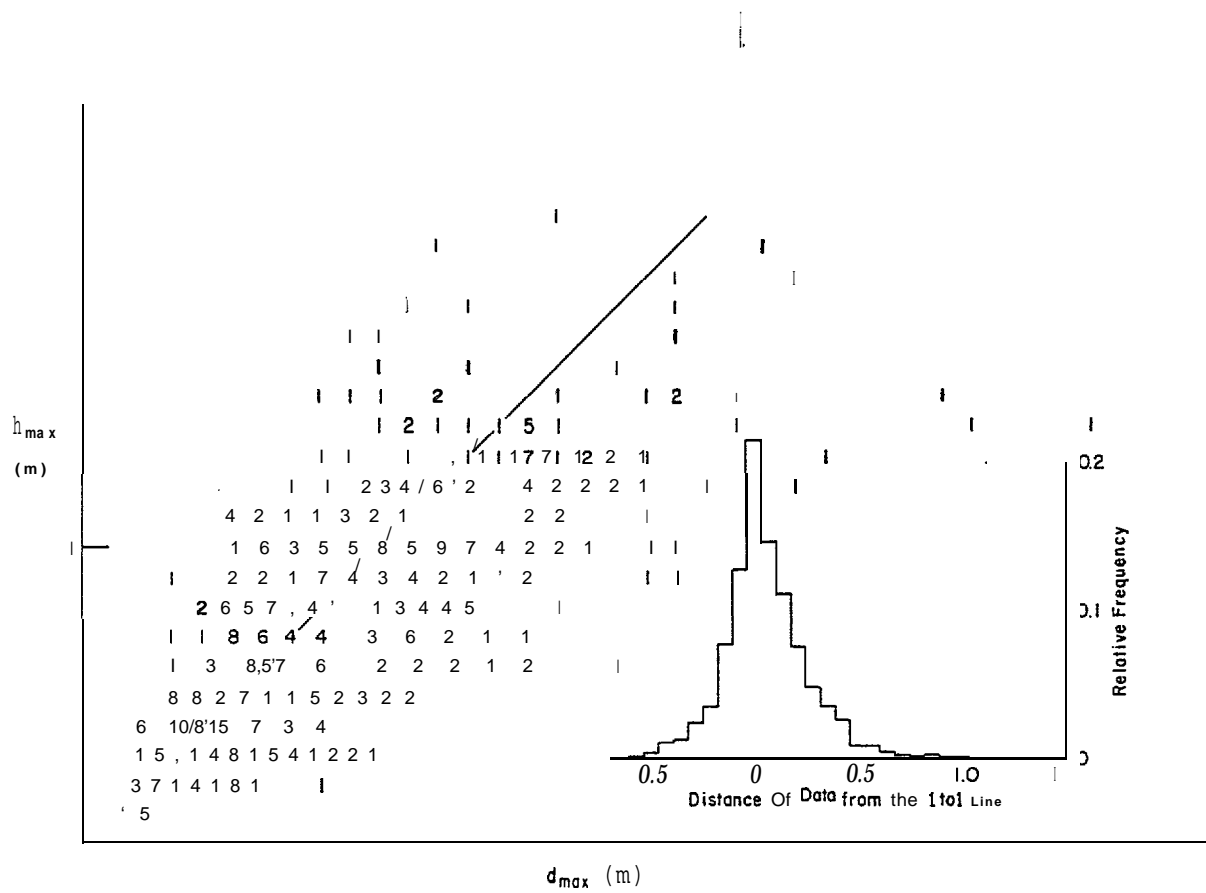


Figure 22. Plot of h_{max} versus d_{max} . Both values are for 1 km line segments. The numbers indicate the number of values present. The inset histogram shows the scatter of the data as measured normal to the 1 to 1 line.

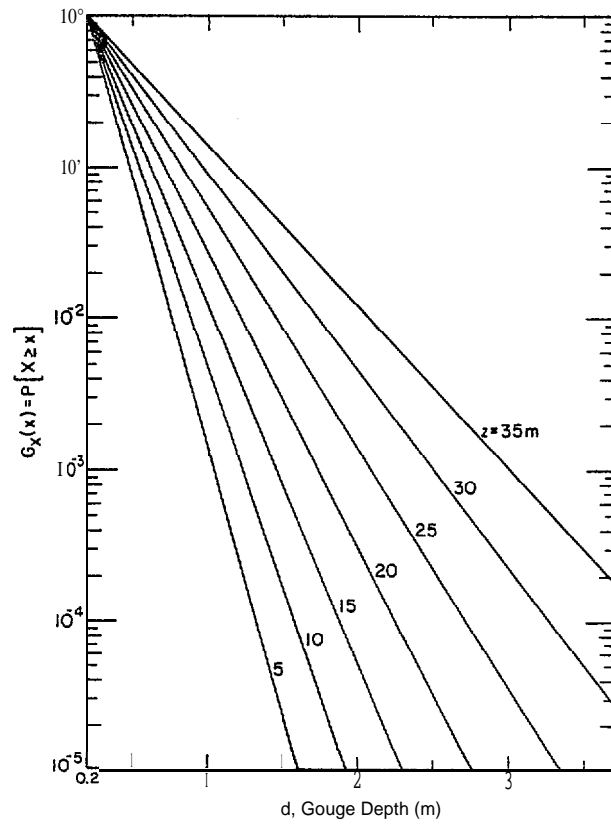


Figure 23. Plot of the exceedance probability ($G_x(x)$) versus gouge depth for different water depths (z) in the offshore region unprotected by barrier islands.

gouges collected over 1500 km of sampling track. In the protected lagoons and sounds, on the other hand, the deepest gouge (0.7 m) was much shallower (from a sample of 41 gouges obtained from 298 km of sampling track) and a large percentage of the 1 kilometer segments examined (92%) contained no gouges at all. In the remainder of this section we will attempt to use the data analysis performed earlier in this paper to make a series of preliminary estimates of the probability of occurrence of gouges with certain prescribed depths and frequencies.

A. Gouge Depths

To obtain the exceedance probability for the occurrence of gouges of different depths given that gouging has occurred, the relation in Figure 10 can be used to obtain an estimate of λ applicable to the water depth of interest. The exceedance probability is then obtained from eq (2). For instance for a water depth of 5 m, $\lambda = 8.16$ and

$$P[D \geq d] = \exp[-8.16(1-0.2)] = 1.46 \times 10^{-3}$$

gives the probability of a gouge exceeding 1 m in depth. Therefore using eq (3) 1 gouge in 685 would be expected to be at least 1 m deep. The 0.2 m correction in the above calculation is caused by the fact that the 0 to 0.2 m depth class was **deleted** in the estimation of λ . At the same water depth 1 gouge in 2.39 million would be expected to be **at least** 2 m deep. For 35 m of water ($\lambda = 2.46$) things are very different, 1 gouge in 7 exceeds 1 m and 1 in 980 exceeds 3 m. A graphical **display** of the variations in the **ex-**ceedance probability as a function of water depth for the offshore region is given in Figure 23.

The λ values determined for lagoons and sounds appear to be in the 7 to 9 m^{-1} range, in short in general agreement with the λ values obtained from similar water depths in the offshore data set.

B. Extreme Value Statistics "

It is important **to** note two factors concerning the extreme values statistics that have been presented. First that the sampling lines cross the gougues at a variety of angles. Therefore from an area where the gouging is spatially homogeneous, in some cases the maximum value used was selected from a small number of gougues (when the sampling line nearly paralleled the gougues) and in other cases from a much large number (when the sampling was perpendicular to the gougues). We have not attempted to correct the extreme value data in the manner that we corrected the observations on the observed number of gougues per kilometer (N) to the number that would be expected if the sampling was perpendicular **to** the gouging (N_1). In fact we do not know how to make such a correction. Secondly it should be realized that the extreme value and the complete distribution techniques give estimates of quite different things. The extreme value approach provides an estimate of the number of 1-km segments that will have at least one gouge greater or equal to some specified value d_{max} along a given length of sampling line. On the other **hand** an estimate using the complete PDF gives the expected number of gougues along the line that are greater or **equal** to d_{max} . The two estimates are not **the** same because a given 1-km sampling segment may have more than one gouge $\geq d_{\text{max}}$. Nevertheless both approaches can be useful if applied appropriately.

Consider three 20 km pipeline routes, one in **the** lagoons and sounds and two at sites unprotected by islands in 5 to **10** and 25 to 30 m of water respectively. For the lagoons and sounds line, the extreme value **exceedance** probability for 1 kilometer sampling intervals is approximately 0.0065 and 0.00013 respectively for gouge depths of 0.5 and 1.0 m corresponding to spatial recurrence intervals of 154 and 7692 km. Corresponding values for 5 to 10 and 25 to 30 m water depths outside of the barrier islands are given in Table 7. Based on this **table** we could conclude that if one was to contemplate using an engineering technique that would encounter difficulties **in** the presence of gouges deeper or **equal** to 1 m, we would not anticipate problems in constructing a 20 km line within **the** lagoons and sounds. On the other hand at water depths **of** 25 to 30 m, we would expect to encounter gouges at least 1 m deep in roughly 15 of the 20 km.

Another parameter of interest is the probability $P(A)$ that the maximum gouge depth per kilometer will equal or exceed a given value (say 1 m) along the pipeline. This is calculated as follows. $P(A)$ equals $1 - P(B)$ where $P(B)$ is the probability that **the** maximum gouge depth per kilometer will not equal or exceed 1 m in any of the 20 kilometers. $P(B)$ in turn equals the probability that the maximum gouge depth per kilometer will not be >1-m in the first kilometer multiplied by the probability that it **will** not be >1 m in the second **kilomter**, etc. Up to the 20th kilometer, Assuming that each kilometer has the same probability $P(C)$ that the maximum gouge depth per kilometer will not **be** >1 m, then $P(B) = [P(C)]^{20}$. $P(C)$ is,

however, equal to 1 minus the probability P(D) that the maximum gouge depth per kilometer will be ≥ 1 m. In short

$$P(A) = 1 - [1 - P(D)]^n \quad (12)$$

where n is the number of 1-km segments composing the line. In our example $n = 20$ and $P(D) = 0.00013$ for lagoons and sounds as that $P(A) = 0.0026$.

These values as well as similar values at water depths of 5 to 10 and 25 to 30 m are also included in Table 7. As is shown the probability of encountering an extreme gouge with a depth equal to or greater than 4 m in water 25 to 30 m deep is appreciably larger than the probability of encountering a 1 m extreme gouge in the lagoons and sounds.

C. Burial Depths

This is a difficult problem that can be considered in several different ways. In such problems it is necessary to use the PDF based on the complete set of gouge depths as opposed to the extreme value distribution based on the maximum gouge in each kilometer. Clearly every gouge greater than a specified value is important.

First we will consider the problem where we wish to bury the pipeline at a depth so that it is all covered (assuming an acceptably low probability of encountering a gouge deeper than our burial depth that would leave the line uncovered). In this case we are dealing with gouge depths as they exist on the sea floor at a given instance of time. Again as an example we will consider a 20 kilometer line that will be, in turn, restricted to lagoons and sounds and the water depths 5 to 10 m and 25 to 30 m outside the barrier islands. We will also consider the case where the direction of the line is 20° off the direction of the gouges as well as

Table 7. **Exceedance** probabilities given 1 km of sample track, spatial recurrence intervals for 1 km segments, and probabilities P(A) that the maximum gouge depth per kilometer will equal or exceed the indicated gouge depth along a 20 km line based on the extreme value statistics.

Location	Gouge depth (m)	Exceedance probability	Spatial recurrence interval (km)	P(A)
Lagoons and Sounds	0.5	0.0065	154.0	0.1223
	1.0	0.00013	7692.0	2.597 $\times 10^{-3}$
Outside barrier islands (water depth 5 to 10 m)	0.5	0.14	7.1	0.9510
	1.0	0.011	90.0	0.1985
	2.0	0.00032	3125.0	6.381 $\times 10^{-3}$
Outside barrier islands (water depth 25 to 30 m)	1.0	0.76	1.3	1.0000
	2.0	0.10	10.0	0.8784
	3.0	0.012	83.0	0.2145
	4.0	0.0018	555.0	0.0354

normal to the direction of the gouges. For instance at a water depth of 25 to 30 m we would expect to encounter an average of 80 gouges per kilometer if the line is normal to the gouges and $80 \sin 20^\circ = 27$ gouges per kilometer if the angle between the gouges and the line is 20° . Considering 20 kilometer lines this corresponds to 1600 and 540 gouges respectively. Next one must decide how many gouges can be tolerated deeper than the depth of burial. We will take two cases: 1 exceedance per 20 km and 1 exceedance per 100 km. Burial depths (x) can then be calculated from eq (3) which when rearranged and modified to treat the above cases becomes

$$\frac{n[D \geq d]}{N} = \frac{n[D > d]}{N_1(\sin\theta)L} = e^{-\lambda(x-0.2)} \quad (13)$$

or rearranging

$$x = \left[\frac{1}{\lambda} \ln \frac{n[D \geq d]}{N_1(\sin\theta)L} \right] + 0.2 \quad (14)$$

As stated, at a water depth of 5 to 10 m, $\lambda = 7.3$, $N_1 = 10$, $\theta = 20$ or 90° , $L = 20$ or 100 km and $n[D \geq d] = 1$ inasmuch as we only wish to allow 1 exceedance. The results of several such calculations are given in Table 8.

Unfortunately the problem we would really like to **solve** is somewhat different and more difficult than the above; a pipeline is buried and we wish to estimate as a function of burial depth how often in a time sense the pipeline can be expected to be impacted by a pressure ridge **keel**. This problem also requires knowledge of the rates of occurrence of new gouges. What **length** of time does the observed gouge sets represent? This question can be examined from several different view points. First, we can estimate

Table 8. Estimated **burial** depths assuming that one existing gouge will exceed the burial depth along **the** length of the **line**.

		Line normal to gouges			Line at 20° to gouges		
	λ (m^{-1})	\bar{N}_1 (gouges/km)	Length of time (km)	Burial Depth (m)	$\bar{N}_1 (\sin 20)$ (gouges/km)	Length of line (km)	Burial Depth (m)
Lagoons and sounds	7.7	0.8	20	0.56	0.27	20	0.42
			100	0.77		100	0.63
Outside the barrier islands (water depth = 5 to 10 m)	7.3	10.0	20	0.93	3.42	20	0.78
			100	1.15		100	1.00
Outside the barrier islands (water depth = 25 to 30 m)	3.2	80.0	20	2.51	27.36	20	2.17
			100	3.01		100	2.67

sedimentation rates in the study area to see how fast gouges would be erased (filled) assuming uniform sedimentation. Average sedimentation rates appear to be quite low. Reimnitz et al. (1977) obtain an average value of 0.06 cm/yr by dividing the observed average thickness of recent (Holocene) sediments (3 m) by the period of time their study area was believed to be covered by the sea (5,000 years). Lewis (1977a) obtained similar but generally higher values (0.05 to 0.2 cm/yr) for his study area north of the Mackenzie Delta. Using the 0.06-cm/yr value and assuming that no other processes are active, it would take about 1666 yrs to fill a 1-m deep gouge and 5000 years to fill a 3-m deep gouge. Based only on this information, an observed gouge set would represent a long period of time.

In the above the assumption of uniform sedimentation on the shelf is probably in error. A gouged bottom morphology creates abrupt local relief and local sedimentation rate anomalies that amount to large differences in sedimentation rates over short distances. Gouge embankments may be sites of erosion while the gouges, as depressions, act as loci of much higher rates of sedimentation than would be apparent on a regional basis. Furthermore, sedimentary structures in shore of 20 m show shelf deposits to consist of gouge in fill material (Barnes and Reimnitz 1974, Barnes et al. 1979).

In addition it is becoming increasingly apparent that shallow water gouges are rapidly obliterated due to high levels of hydrodynamic activity (Kovacs 1972, Pilkington and Marcellus 1983). For instance, recent field observations of Barnes and Reimnitz (1979) show that the extensive open-water conditions that occurred during the summer of 1977 resulted in

hydrodynamic conditions (presumably, large waves and wind-generated shelf currents associated with the presence of a large fetch) that have obliterated ice gouges to a water depth of 13 m, and caused pronounced **infilling** of ice gouges in deeper water. Apparently, the rates of reworking and redepositing sediment from such episodic events are much larger than the average sediment accumulation rate on the Beaufort Sea **shelf**. We know of no studies of the recurrence frequency of conditions such as **those** observed during the summer of 1977 but we would guess that they are fairly common with return periods of no more than 25 years. Twenty-five years appears to be a reasonable estimate for the return period of significant storm surges along the coast of the Beaufort Sea (**Reimnitz** and Maurer 1978); events that would presumably be associated with similar or more energetic hydrodynamic conditions. In short although sedimentation rates might **lead** one to believe that the Beaufort Shelf **is** a rather static environment **sedimentologically**, this is far from the case, and this comment is particularly true in locations where water depths are less than 10 meters. Therefore, in most of the area we have studied, we would not have confidence in the assumption that the sea floor, as seen at a given time, represents a steady state condition with the number **of** new scours per unit time **equalling** the **number** of scours **infilled by** sedimentation plus the number of new scours superimposed **on** existing scours. Such statistical time invariance of the gouging is an essential assumption if the rate of production of **new** gouges is estimated using the scour budget approach developed by Lewis (1977a, **b**). We think the method is interesting and quite possibly applicable to certain regions of gouging, for instance

offshore areas in the **Chukchi** Sea with water depths of 30 to 50 m. However for the Beaufort Sea in general, and in particular for water depths less than 20 m, we **feel** that the applicability of the steady state assumption is doubtful.

Another approach used to get a rough estimate of the age of an observed set of gouges is to divide the average value for the annual sum of the gouge widths by the length of the sample track (**Reimnitz** et al. 1977a). For instance, if our sample line is 10 km long and we obtain an average of 500 m of new gouges crossing the line each year, we then take 20 years as an estimate of the time period in which the gouges are completely replaced. In fact, such estimates give the shortest period of time in which the gouge set **could** be replaced (an event of very low probability) as ice presumably plows the sea **floor** in a random (**not** a systematic) manner. Therefore, the fact that a given segment of a line has just been gouged has no effect on the probability that the segment **will** be gouged the next year (or the next month).

Still another approach using the same data set assumes that an increasingly large proportion of the bottom is **regouged** before the entire bottom is gouged (**Barnes et al.** 1978). In this scheme if 10% of the seabed is gouged each year then in the first year 10% is impacted with new gouges but in the second year only 19% is gouged as 1% of the gouges occurred in areas already gouged. This can be expressed as the polynomial

$$G_t = 1 - (1 - K)^T \quad (15)$$

where G_t is the fraction of **the** bottom gouged since T_0 , K is the fraction of the bottom gouged each year and T **is** the time in years measured relative to T_0 .

Finally attempts have been made to combine information on pressure ridge keels, pack **ice** drift **and** observed distributions of scour depths **to** estimate required burial depths (**Pilkington and Marcellus 1981, Wadhams, in press**). As the first two of these parameters are very poorly known, such estimates are **highly** uncertain. This technique also appears to give maximum gouge depths that are appreciably deeper than observed. More will be said about this later.

We believe that at present to adequately examine the pipeline burial problem independent information on gouging rates and the depths of recent gouges is essential. As we have described, our information on this subject is hardly what we would desire. Nevertheless it is enough **to allow us to** make an initial approach to estimating burial depths. To summarize our recent gouge observations on recent gouges we found that \bar{g} , the number of gouges per km per year varied from 2.4 to 7.9 with a mean of 5.2. There also was no apparent relation between g and water depth. The PDF for recent gouges was exponential with a **value** of 4.5 m^{-1} , a value that is **1** m^{-1} less than comparable values from **all** the gouges existing on the sea floor at a given time.

Using this information we can now make preliminary estimates of the burial depths required so that a pipeline of a given length **will**, on the average, be **gouged** once during a specified period of time (**for instance 1** time in 100 or **in** 1000 years). To do this, first estimate N , the total

number of gouges that will occur during the proposed lifetime of the pipeline by

$$N = \bar{g} T L \sin \theta \quad (16)$$

where \bar{g} is the average number of gouges/km/year occurring along the pipeline route, T is the proposed lifetime in years, L is the length of the line in kilometers, and θ is the angle between the route and the trend of the gouges. As we only consider 1 contact in T, $n[D \geq d]$ in eq (3) equals 1 and we obtain

$$e^{-\lambda(x-0.2)} = \frac{1}{\bar{g} T L \sin \theta} \quad (17)$$

or

$$x = \left[-\frac{1}{\lambda} \ln \frac{1}{\bar{g} T L \sin \theta} \right] + 0.2 \quad (18)$$

In Table 9 we show a series of burial depth estimates made using eq {18}. In these calculations we have used both the observed value for the existing gouge set from Figure 10 and also -1 as an estimate of the corresponding parameter for new gouges. In using the table note that a 20 year lifetime for a 100 km line is identical with a 100 year lifetime for a 20 km line. As can be seen in the table, it is very important to obtain data that will allow improved estimates of λ and \bar{g} for new gouges. In general it can be said that slight increases in the burial depth (a few tens of centimeters) result in appreciable increases in the safety of the

Table 9. Estimated burial depths assuming 1 contact between a pressure ridge **keel** and the pipeline during the lifetime of the pipeline (taken as 100 years). Calculations made using eq (18).

Location	\bar{g} (gouges/km/ year)	λ or $(\lambda-1)$ (m-')	Length of line (km)	Line normal to gouges		Line at 20° to gouges	
				Gouges crossing line during 100 yr lifetime	Burial depth (m)	Gouges crossing line during 100 yr lifetime	Burial depth (m)
Lagoons and sounds	5	7.7	20	10,000	1.40	3,420	1.26
		7.7	100	50,000	1.61	17,101	1.61
		6.7	20	10,000	1.57	3,420	1.41
		6.7	100	50,000	1.81	17,101	1.81
Outside the barrier islands (water depth = 5 to 10 m)	5	7.3	20	10,000	1.46	3,420	1.31
		7.3	100	50,000	1.68	17,101	1.54
		6.3	20	10,000	1.66	3,420	1.49
		6.3	100	50,000	1.92	17,101	1.75
Outside the barrier islands (water depth = 25 to 30 m)	5	3.2	20	10,000	3.08	3,420	2.74
		3.2	100	50,000	3.58	17,101	3.25
		2.2	20	10,000	4.39	3,420	3.90
		2.2	100	50,000	5.12	17,101	4.63

line. This statement is particularly true in shallow water where λ is **large.**

In Table 10 we have also included a comparison between our estimates of burial depths and those of **Wadhams** (in press) for a 76 km line (the distance from the artificial gravel island "**Kopanoar**" to the shore), The return period for an impact is taken *to be* 1000 years. There are large differences in the estimates with our burial depths being roughly 3 m less than **Wadhams**. In fact for the 25 m water depth our estimates would only be 4.05 and 5.47 m (assuming $\lambda = 3.7$ and **2.7** respectively} if we took \bar{g} to be 20; a value 4 times that observed. We believe the difficulty with **Wadhams** approach lies not in its principles but in the difficulty in obtaining appropriate values to use in the theory. For instance keel depth characteristics in deeper water where it is possible to probe the underside of the ice via submarine are probably appreciably different from that in water of 50 m or less where gouging **is** currently taking **place**. **Also it is,** at present, particularly difficult to know what values to assume for the distance drifted per year by the ice cover over a given point. When gouging starts the ice is slowed and many times stopped as the grounded ice tends to stabilize the nearby pack converting it to fast ice.

IX. CONCLUSION

In this paper we have presented a **large** amount of data on the statistical characteristics of the ice-produced gouges that occur on the Alaskan shelf of the **Beaufort** Sea **in** shallow water (<38 m). Although at first glance the gouges appears to be rather chaotically distributed, in a statistical sense they are very systematic. Consequently we have used this information to estimate the requisite burial depths of pipelines that **would**

Table 10. Comparisons between burial depths to the top of a 76 km pipeline for a 1000 year return period as calculated using eq (18) and-by Wadhams (in press).

Water depth (m)	\bar{g}	λ or $(\lambda-1)$ (m^{-1})	Burial depth (m)	Source
15	5	5.5	2.54	This paper (eq 18)
	5	4.5	3.06	This paper (eq 18)
	10	5.5	2.66	This paper (eq 18)
	10	4.5	3.21	This paper (eq 18)
15			6.24	Wadhams (in press)
25	5	3.7	3.67	This paper (eq 18)
	5	2.7	4.96	This paper (eq 18)
	10	3.7	3.86	This paper (eq 18)
	10	2.7	5.22	This paper (eq 18)
25			8.10	Wadhams (in press)

allow one hit by an ice mass in a specified number of years.

In conclusion we would like to comment on some problems that, if properly studied, would contribute to the understanding of the geophysics of gouging and to the safe design of sea floor pipelines in regions where gouging is known to occur. We believe the weakest link in the present study is the paucity of information on the rate of occurrence of new gouges and their characteristics. Field programs should be expanded to collect this type of information. In areas where offshore development is contemplated, it is important to start studies of gouging rates as soon as possible, as the collection of an adequate data set takes several years.

Systematic regional sampling is also required to reveal changes, if any, in the probability density functions of parameters such as gouge depth with changes in location and in environment on **the** shelf. Current information suggests that there are appreciable changes in such parameters on a regional **scale** (for instance between the gouge depths in the present study area and those observed off the Mackenzie Delta). Studies should also be carried out to quantify the effects of differences in slope angle and aspect and of the nature of bed material on gouging. Such work in conjunction with detailed site-specific studies would be very useful in evaluating hazards along specific pipeline routes.

Theoretical studies should also be implemented to advance our ability to treat gouging as a stochastic process. For instance it would be useful to look at gouging as a simple covering problem in geometric probability.

If such developments are sufficiently general, they can be applied to different geographic areas by simply changing the values of the input parameters.

Finally, it would be useful to improve **our** understanding of the interactions between pressure ridge and ice island keels and the sea floor. Perhaps such studies will provide insight into the possibility of determining maximum probable gouge depths for a given sediment type. until such information is available we can only assume that even apparently "impossibly" deep gouges have a finite probability of occurrence.

REFERENCES

- APO - Alaskan Projects Office (1978) Environmental Assessment of the Continental Shelf, Interim Synthesis: **Beaufort/Chukchi**. Outer Continental **Shelf** Environmental Assessment Program, NOAA, Environment Res. Laboratories, Boulder, Colorado.
- Barnes, **P.W.** and D. McDowell (1978) New bathymetric map of the Alaskan Beaufort Sea. Environmental Assessment of the Alaskan Continental Shelf, Quarterly Reports of Principal Investigators, April-June 1978, vol. , p. 267-9 and Fig. 1.
- Barnes, **P.W.** and E. **Reimnitz** (1974) Sedimentary processes on Arctic shelves off the north coast of Alaska. In "The Coast and **Shelf** of the Beaufort Sea" (**J.C. Reed** and **J.E. Sater**, eds.) Arctic Inst. North America, Arlington, Virginia, p. 439-76.
- Barnes, **P.W.** and E. **Reimnitz** (1979) Ice gouge obliteration and sediment redistribution event; 1977-1978, **Beaufort** Sea, Alaska. U.S. Geological Survey Open **File** Rept 79-848, 22 p.
- Barnes, **P.W.**, D. McDowell and E. **Reimnitz** (1978) Ice gouging characteristics: their changing patterns from 1975-1977, Beaufort Sea, Alaska. U.S. Geological Survey Open File Rept. 78-730, 42 pp.
- Barnes, **P.W.**, E. **Reimnitz**, **L.J. Toimil**, **P.K. Maurer** and D. McDowell (1979) Core descriptions and preliminary observations of **vibracores** from the Alaskan Beaufort Sea shelf. U.S. Geological Survey Open File Report 79-351, 106 pp.
- Benjamin, **J.R.** and **C.A. Cornell** (1970) Probability, Statistics and Decision for **Civil** Engineers. McGraw-Hill, New York, 684 pp.
- Fredsoe, J. (1979) Natural backfilling of pipeline trenches. Journal of Petroleum Technology, October, p. 1223-30.
- Haan, **C.T.** (1977) Statistical Methods in Hydrology. The Iowa State University Press, Ames, 378 pp.
- Hahn, **G.J.** and S.S. Shapiro (1967) Statistical Models in Engineering, Wiley and Sons, New York, 355 pp.
- Hnatiuk**, J. and **K.D. Brown** (1977) Sea bottom scouring **in** the Canadian Beaufort Sea. 9th Annual Offshore Technology Conference, Houston, Texas, Paper OTC 2946, p. 519-27.
- Hopkins, **D.M.** (1967) The **cenozoic** history of **Beringia** - A synthesis. **In** The Bering Land Bridge (**D.M. Hopkins**, cd.), Stanford University Press, Stanford, California, p. 451-84.

- Kindle, **E.M.** (1924) Observations on **ice-bourne** sediments by the Canadian and other arctic expeditions. *American Journal of Science* 7, 251-86.
- Kovacs, A.** (1972) Ice scoring marks floor of the Arctic shelf. *The Oil and Gas Journal* 70 (23 Oct. 1972), p. **92-106.**
- Kovacs, A. and M. **Mellor** (1974) Sea ice morphology and ice as a geologic agent in the southern Beaufort Sea. In "The Coast and Shelf of the Beaufort Sea" (**J.C. Reed and J.E. Sater, eds.**), Arctic Inst. North America, Arlington, Virginia, p. 113-161.
- Lewis, **C.F.M.** (1977a) Bottom scour by sea ice in the southern Beaufort Sea. Dept. of Fisheries and the Environment, Beaufort Sea Technical **Rept.** 23 (draft), Beaufort Sea Project, Victoria, British Columbia, 88 pp., [copies available from the author].
- Lewis, **C.F.M.** (1977b) The frequency and **magnitude of drift ice groundings** from ice-scour tracks in the Canadian Beaufort Sea. In "Proceed. 4th Internat. Conf. Port and Ocean Engineering Under **Arctic** Conditions **Memorial** University, Newfoundland, **vol. 1**, p. 567-76.
- Mardia, **K.V.** (1972) Statistics of Directional Data. Academic press, New York, 357 pp.
- Mathews, **J.B.** (1981) Observations of surface and bottom; currents in the Beaufort sea near Prudhoe Bay, Alaska. Journal of Geophysical Research, **86(C7)**, 6653-60.
- Miller, **I.** and Freund, **J.E.** (1977). Probability and Statistics for Engineers, Prentice-Hall.
- Pelletier, B.R.** and Shearer, **J.M.** (1972) Sea bottom scouring in the Beaufort Sea of the Arctic Ocean. 24th International **Geol.** Congress, Sect, 8, Marine Geology and Geophysics, Montreal, p. 251-61.
- Pilkington, G.R.** and **R.W. Marcellus** (1981) Methods of determining pipeline trench depths in the Canadian Beaufort Sea. In "POAC 84'* Proceedings, the 6th International Conference, Vol. II, p. **674-87.**
- Rearic, D.M., P.W. Barnes** and **E. Reimnitz** (1981) Ice-gouge data, Beaufort Sea, Alaska, 1972-1980. U.S. Geological Survey Open File Report 81-950.
- Reimnitz, E. and **P.W. Barnes** (1974) Sea ice as a geologic agent on the Beaufort Sea shelf of Alaska. In "The Coast and Shelf of the Beaufort Sea" (**J.C. Reed and J.E. Sater, eds.**) Arctic Inst. North America, Arlington, Virginia, p. 301-353.
- Reimnitz, E.** and **D.K. Maurer** (1978) Storm surges in the Alaskan Beaufort Sea. U.S. Geological Survey Open-File Report 78-593, 26 pp.

- Reimnitz, E., P.W. Barnes, T.C. Forgatsch, and C.H. Rodeick, (1972) Influence of grounding ice on the Arctic shelf of Alaska. *Marine Geology*, 13, 323-34.
- Reimnitz, E., P.W. Barnes and T.R. Alpha (1973) Bottom features and processes related to drifting ice on the Arctic shelf, Alaska. U.S. Geological Survey Misc. Field Studies Map **MF-532**.
- Reimnitz, E., P.W. Barnes, L.J. Toimil, and J. Melchior (1977a) Ice gouge recurrence and rates of sediment reworking, Beaufort Sea, Alaska. *Geology* 5, 405-8.
- Reimnitz, E., L.J. Toimil, and P.W. Barnes (1977b) **Stamukhi** zone processes: implications for developing the Arctic Offshore. 9th Annual Offshore Technology Conference, Houston, Texas, Paper OTC 2945, p. 513-18.
- Reimnitz, E., L.J. Toimil and P.W. Barnes (1978) Arctic continental shelf morphology related to sea-ice **zonation**, Beaufort Sea, Alaska. *Marine Geology* 28, 179-210.
- Shearer, J.M. and S.M. Blasco (1975) Further observations of the scouring phenomena in the Beaufort Sea. In "Report of Activities, Part A, Geological Survey of Canada, Paper 75-1A, 483-93.
- Shearer, J.M., E.F. MacNab, B.R. Pelletier and T.B. Smith (1971) Submarine pingos in the Beaufort Sea. *Science* 174, 816-8.
- Skinner, B.C. (1971) Investigation of ice **island** scouring of the northern continental shelf of Alaska. U.S. Coast Guard Acad. Rept. RDC GA-23, 24 p.
- Slack, J.R., J.R. Wallis and N.C. Matalas (1975) On the value of information to flood frequency analysis. *Water Resources Research*, Vol. 11, p. 629-47.
- Thomas, D.R. and R.S. Pritchard (1979) Beaufort and **Chukchi** Sea Ice Motions. Part 1. Pack ice trajectories. FLOW Research Report No. 133, FLOW Research Company, Kent, Washington.
- Tucker, W.B., W.F. Weeks and M.D. Frank (1979) Sea ice ridging over the Alaskan continental shelf. *Journal of Geophysical Research*, Vol. 84(C8), p. 4885-97.
- USWRC (1977) Guidelines for Determining Flood Flow Frequency. Bulletin 17A of the Hydrology Committee. United States Water Resources Council, Washington, D.C. 163 pp.
- Wadhams, P. (in press) Predictions of extreme keel depth from submarine sonar data. Cold Regions Research and Engineering.

Wahlgren, R.V. (1979a) Ice-scour tracks on the Beaufort Sea continental shelf - their form and an interpretation of the processes creating them. M.A. Thesis, Dept. of Geography, Carleton University, Ottawa, 183 p.

Wahlgren, R.V. (1979b) Ice-scour tracks in eastern Mackenzie Bay and north of Pullen Island, Beaufort Sea. In Current Research, Part B, Geological Survey of Canada, Paper 79-1B, 51-62.

•

Figure Captions

Figures

1. Map of a part of the Alaskan coastline of **the** Beaufort Sea giving place names mentioned in text.
2. Generalized bathymetric chart of the study area.
3. **Sonograph** of ice gouged seafloor, Water depth is **20 m**. Record taken **20 km** NE of Cape **Halkett**.
4. Fathogram of ice gouged seafloor. Wate depth **is 36 m**. Record taken **25 km** NE of Cape **Halkett**.
5. Map showing the location of the sampling lines. The arrows indicate the direction of ship movement.
6. Schematic drawing of a gouge showing the locations of several measurements referred to in the text.
7. **Semilog** plot of the number of gouges observed versus gouge depth for 4 regions along the Alaskan coast of the Beaufort Sea.
8. **Plot** of λ (m^{-1}) versus water depth (z) in meters for 4 different geographic areas along the coast of the Beaufort Sea.
9. Relative frequency of occurrence of gouges of differing depths based on all data from "offshore" areas unprotected by barrier islands.
10. λ values (m^{-1}) versus water depth (m) based on the data set from "offshore*" areas unprotected by barrier islands.
11. Linear histograms of the observed probability of different dominant gouge orientations.
- 12* Number of gouges per kilometer measured normal to the trend of the **gouges** (N_1) versus water **depth** (m).

13. Relative frequency of different **values** of $N_1/10$ for **lagoons** and sounds and 3 different water depths offshore of the barrier islands.
14. Frequency of occurrence versus the observed distances between the gouges off Lonely, Alaska.
15. Number of gouges/km/yr (g) versus water depth (m).
16. Relative frequency of different values of g (number of **gouges/km/yr**). The discrete distribution is a fitted Poisson and the stippled distribution is a fitted Gamma.
17. Semi-log plot of the relative frequency of occurrence of new gouges of differing depths (m).
18. plots of d_{\max} versus water depth (z)—for 5 different regions within the study area.
19. **Exceedance** probability per km of sample track for different water depths versus d_{\max} . The horizontal lines represent the locations of a number of data points (as the data were grouped in class intervals there commonly are several values of the exceedance probability with the same d_{\max} (the midpoint of the class interval)).
20. Parameters relating to the determination of eq (11) shown as a function of water depth (\bar{z}).
21. Plot of w_{\max} for 1 km line segments versus water depth (\bar{z}) for **all** locations except those from lagoons and sounds.

22. Plot of h_{\max} versus d_{\max} . Both value are for 1 km line segments. The numbers indicate the number of values present. The inset histogram shows the scatter of the data as measured normal to the 1 to 1 line.
23. Plot of the exceedance probability ($G_X(x)$) versus gouge depth for different water depths (z) in the offshore region unprotected by barrier Islands.

Tables

1. Summary of gouge depth (d) measurements.
2. Descriptive statistics on the variation in the dominant orientations of the gouges.
3. Summary of the observations on the number of gouges (deeper than 0.2 m) per kilometer.
4. Parameters of gamma distributions fitted to observational data on the number of gouges per kilometer.
5. Number of new gouges during the indicated time and space intervals. The 1973-5 and 1975-6 data are from Names et al. 1978).
6. Parameters of the log Pearson type III distribution determined from the maximum gouge depths observed along 1-km sampling lines.
7. Exceedance probabilities given 1 km of sample track, spatial recurrence intervals for 1 km segments, and probabilities that the maximum gouge depth per km will equal or exceed the indicated gouge depth along a 10 km line.
8. Estimated burial depths assuming that one existing gouge will exceed the burial depth along the length of the line.

9. Estimated **burial** depths assuming 1 contact between a pressure ridge keel and the pipeline during the lifetime of the pipeline (taken as 100 years).
10. Comparisons between burial depths to the top of a 76 km pipeline for a 1000 year return period as calculated using eq (18) and by **Wadhams** (in press).